View Article Online
View Journal

Dalton Transactions

An international journal of inorganic chemistry

Accepted Manuscript

This article can be cited before page numbers have been issued, to do this please use: S. Dey, D. Buzsaki, C. Bruhn, Z. Kelemen and R. Pietschnig, *Dalton Trans.*, 2020, DOI: 10.1039/D0DT00941E.

ROYAL SOCIETY OF CHEMISTRY

rsc.li/dalton

View Article Online
DOI: 10.1039/D0DT00941E

ARTICLE

Bulky 1,1'-bisphosphanoferrocenes and their coordination behaviour towards Cu(I)

Received 00th January 20xx,
Accepted 00th January 20xx

DOI: 10.1039/x0xx00000x

Subhayan Dey,[†] Daniel Buzsáki,[‡] Clemens Bruhn,[†] Zsolt Kelemen*[‡] and Rudolf Pietschnig*[†]

Two bulky mesityl substituted dppf-analogs $Fe(C_5H_4PMes_2)_2$ (Mes = 2,4,6-$Me_3C_6H_2$, **1**) and $Fe(C_5H_4PMes_2)(C_5H_4PPh_2)$ (Mes = 2,4,6-$Me_3C_6H_2$, Ph = C_6H_5, **3**) have been prepared and their properties as donor ligands have been explored using heteronuclear NMR spectroscopy and in particular via the $^1J_{P\text{-}Se}$ coupling, cyclic voltammetry and DFT calculations. Based on these results, a series of mono and dinuclear Cu(I) complexes have been prepared with these new diphosphane ligands using Br^-, I^-, BF_4^- as counter anions. For the very bulky ligand **1** rare and unprecedented double bridging complexation modes have been observed containing two non-planar Cu_2Br_2 units, while for the other dinuclear complexes planar Cu_2Br_2 units have been found. The Cu(I) complexes of **1** and **3** were then used as catalysts for CO_2-fixation reaction with terminal alkyne, where complexes with ligand **3** were found more efficient than those with **1**. DFT calculations performed on compounds **1**, **3** and their Cu(I) complexes were able to verify the trend of these catalytic reactions.

Introduction

Being an extremely useful and unique building block, ferrocene remains a center of attraction for several decades now. Apart from the fact that it is important for synthesizing organometallic polymers,[1-5] preparing redox-tunable substances,[4, 6-8] drug discovery,[9, 10] and fabrication of other functional materials,[11-14] ferrocene has played a vital role in homogenous catalysis.[15, 16] When the diphosphane ligand-systems emerged from their mono-phosphane counterparts, ferrocene provided them with an unprecedented backbone,[17-19] which helped to stabilize variety of metal centers by attaining flexible geometries.[15, 20] This special arrangement has further been appreciated, when it emerged that the bite angles (β_n, **A**, Figure 1) of such ligands, which have an apparent positive effect on the efficiency of catalysts,[21, 22] can be manipulated by changing the substituents on phosphorus.[23] Systematic investigations further revealed that the alteration of substituents on phosphorus can be achieved by simple and modular synthetic approaches.[23, 24] The aforementioned qualities made ferrocene-based diphosphane ligands remarkably successful for homogenous catalysis.[15, 16] The quest for new ligands, with ideal steric demand and optimum donating ability, is still relevant to date.[25-30]

Although many different 1,1'-symmetrically and unsymmetrically substituted bisphosphanoferrocenes have been reported in the past (**B** and **C**, Figure 1),[19, 23, 25, 31-40] the catalytic discussions were dominated by 1,1'-bis(diphenylphosphano)ferrocene (dppf, **D**, Figure 1) for many decades.[15, 16, 24] However, in 2007, it has been reported that 1,1'-bis(di-tert-butylphosphano)ferrocene (dtbpf, **E**, Figure 1) is superior to dppf for the Pd-catalyzed α-arylation of ketones and certain Pd-catalyzed Suzuki coupling reactions.[41, 42] Moreover, in the recent past, several reports have theoretically proven the fact that with the increase of the steric bulk on phosphorus, the donating ability and β_n increase, and as a result increases the catalytic activity.[43, 44] In this context, two obvious questions arise: 1) What is the maximum attainable steric before the complexation of 1,1'-bisphosphanoferrocene compromises? 2) How much steric bulk can be used without harming the catalytic activity of the resulting complexes? Since the steric situation will differ from one metal to the other, we have explored a catalytic process and addressed the previous questions with the help of two novel sterically congested 1,1'-diphosphanoferrocene ligands, namely 1,1'-bis(dimesityl-phosphano)ferrocene and 1-(dimesitylphosphano)-1'-(diphenyl-phosphano)ferrocene. The complete syntheses of these ligands, their electrochemical properties and donating abilities will be investigated herein, as well as a first insight into their potential in catalysis.

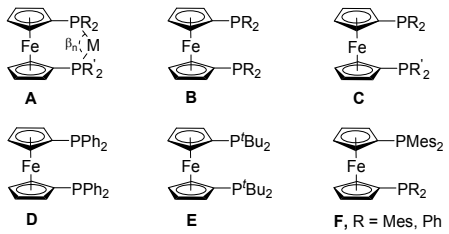

Fig 1. Bite angle (β_n, **A**),[21, 22] previously (**B**-**E**),[23] and herein reported (**F**) achiral 1,1'-bisphosphanoferrocene ligands. Known symmetrically substituted dppf analogs (**B**): R = Me,[17] Et,[34] *i*Pr,[31, 45] Cy,[19] *t*Bu,[32] *o*-tolyl,[33, 46] *o*-MeO-C_6H_4,[34] *p*-MeO-C_6H_4,[47] *p*-PhO-C_6H_4,[46] *p*-CF_3-C_6H_4,[48] 3,5-CF_3-C_6H_3,[33] 2-furyl,[33] 5-Me-2-furyl,[37] *o*-*i*Pr-C_6H_4,[34] 1-Nap,[46] 2-Nap,[46] C_6F_5.[34] Known 1,1'-unsymmetrically

[†] *Institut für Chemie und CINSaT, University of Kassel, Heinrich Plett-Straße 40, 34132 Kassel, Germany*
[‡] *Department of Inorganic and Analytical Chemistry, Budapest University of Technology and Economics, and MTA-BME Computation Driven Chemistry Research Group, Szent Gellért tér 4, 1111 Budapest, Hungary.*
Electronic Supplementary Information (ESI) available: NMR spectra, crystal structures of **4** and **6**, crystal refinement data, CV and Details of DFT calculations. See DOI: 10.1039/x0xx00000x

substituted dppf analogs (**C**): R = Ph, R' = ^{t}Bu;[35, 36] R = Ph, R' = ^{i}Pr;[25] R = Ph, R' = Cy;[25] R = Ph, R'= *p*-MeO-C_6H_4;[38] R = Ph, R'= 5-Me-2-furyl;[37] R = Ph, R'= Cl;[39] R = Ph, R'= OPh;[40] R = Ph, R'= OMen;[39] R = Ph, R'= *p*-Me-Ph;[38] R = *p*-Me-Ph, R'= *p*-CF_3-Ph.[38]

Owing to the current interest in using CO_2 as sustainable feedstock in catalytic transformations, we set out to investigate the catalytic formation of propiolic acid derivatives from CO_2 and terminal alkynes. The first report of such catalytic CO_2-fixation reaction was published by the Inoue group in 1994, where CuI was used as catalyst (Scheme 1a).[49] Although insertion of CO_2 into alkynylcopper was successful, high temperature and a large excess of base were needed for the execution of this reaction.[49, 50] Recently, Rath *et. al.* has reported the similar carboxylation reactions with Cu-complexes of dtbpf, where ambient temperature have been used for high yielding transformations (Scheme 1b).[51] Considering the fact that copper is an affordable late transition metal and potentially active for the reaction of our interest,[50, 52, 53] we first decided to synthesize the CuX (X = Br, I, $(MeCN)_nBF_4$) complexes of our ligands. The structural properties of these complexes and their catalytic behaviour have further been studied in this report. Finally, to take an insight into the energetic scenario of complexation and the related catalysis, we have used density functional theory (DFT), which further helped us to verify the experimentally obtained results.

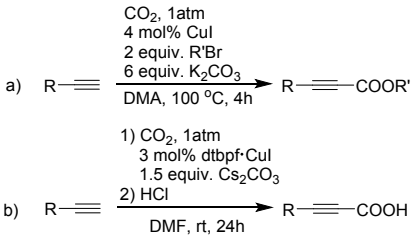

Scheme 1. Cu-catalyzed carboxylation of terminal alkynes.[50]

Result and Discussion

Syntheses and Complexation

A few 1,1'-substituted ferrocenyl compounds, with two dimesitylphosphanyl groups were previously synthesized by reacting modified dilithoferrocene with Mes_2PCl as reagents (**G**, **H**, **I**, Scheme 2).[54, 55] However, their properties as bidentate ligands in metal complexation and homogenous catalysis have not been explored in detail, except for a few instances of silver-mediated nucleophilic fluorination.[55]

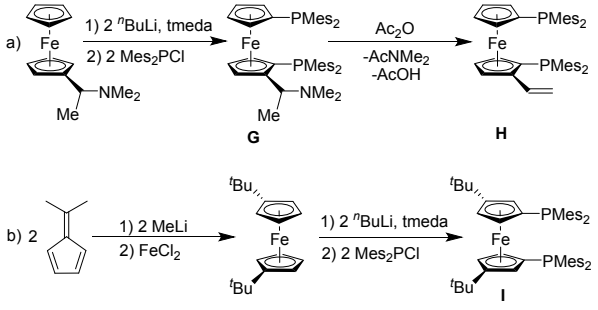

Scheme 2. Syntheses of substituted 1,1'-bis(dimesitylphosphano)-ferrocenes.[54, 55]

The synthesis of our mesityl-substituted bisphosphano ligand **1** was carried out by two complementary pathways. The first pathway involves PCl_2-substituted ferrocene **2**, which was synthesized by a known method,[56, 57] and subsequently reacted with four equivalents of MesLi·LiBr·OEt_2 (Scheme 3a). On the other hand, the second pathway (Scheme 3b) uses tmeda-stabilized dilithioferrocene, which was reacted with two equivalents of Mes_2PX (X = Cl, Br). Although both the pathways can produce **1** in an acceptable purity, the first pathway (Scheme 3a) gives slightly higher yield than the second (Scheme 3b).

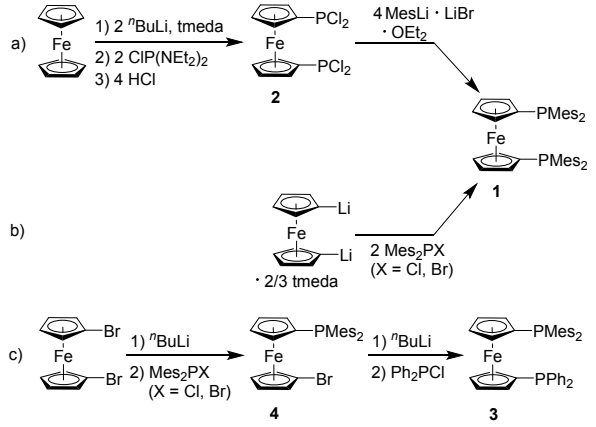

Scheme 3. Syntheses of mesityl-substituted bisphosphano ligands **1** and **3**.

The unsymmetrically substituted bisphosphano ligand **3** was synthesized by following a simple and modular approach (Scheme 3c). At first, compound **4** was synthesized by selective monolithiation of 1,1'-dibromoferrocene,[58] and subsequent in situ reaction with Mes_2PX. When compound **4** was further monolithiated and in situ reacted with Ph_2PCl, compound **3** was obtained in an overall yield of 33%, starting from 1,1'-dibromoferrocene.

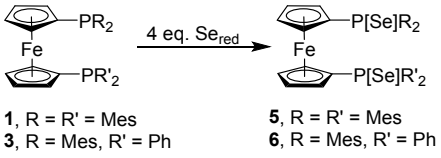

Scheme 4. Syntheses of diselenide derivatives of **5** and **6**.

In order to explore the donating abilities of our ligands, the selenophosphorane derivatives of **1** and **3** were synthesized by adapting a reported procedure (Scheme 4), and their $^1J_{P\text{-}Se}$ values were compared with selenides of other phosphane ligands.[59, 60] Since compounds **5** and **6** are not soluble in common NMR solvents like $CDCl_3$ and C_6D_6, our comparison became restricted to data available for toluene solutions. To this end we recorded ^{31}P and ^{77}Se NMR spectra of $Ph_3P[Se]$ and $dppf[Se]_2$ in toluene as benchmark for this comparison as well, since the underlying phosphanes Ph_3P and dppf are extremely popular and useful ligand in many synthetic applications.[15, 16, 61-77] The $^1J_{P\text{-}Se}$ for compound **5** (723 Hz) is significantly lower than the corresponding values for $Ph_3P[Se]$ (732 Hz in $CDCl_3$;[78] 758 Hz in toluene-d8, see Figure S61 in SI file), and $dppf[Se]_2$ (737 Hz in $CDCl_3$;[59, 79] 761 Hz in toluene-d8, see Figure S59 in SI file), which indicates that the lone pairs of phosphorus centres in **1** have a lower *s* character, and therefore, higher donating ability than Ph_3P and dppf. A similar trend could also be noticed for the ^{77}Se NMR chemical shifts, where the resonance of compound **5** at -82

ppm is deshielded by ca. δ 200 ppm and 220 ppm, compared to $Ph_3P[Se]$ and $dppf[Se]_2$, respectively (see Figures S21, S62 and S60 in SI file), which is in fact closer to values observed for the selenides of push pull substituted phosphane.[60]

In line with the lower symmetry in compound **6**, two different values for $^1J_{P\text{-}Se}$ have been observed: 723 Hz for $Mes_2P[Se]$ and 763 Hz for $Ph_2P[Se]$, which are coherent with the corresponding values of **5** and $dppf[Se]_2$, respectively. The ^{77}Se NMR spectra of compound **6** shows a set of two doublets, for the Se atoms at the two different phosphorus centres at -78 ppm ($PSeMes_2$) and -299 ppm ($PSePh_2$), which are consistent with the values observed for **5** and $dppf[Se]_2$ (see Figures S21, S25 and S60 in SI file). It should be noted that although the $^1J_{P\text{-}Se}$ values for $dtbpf[Se]_2$,[80] $dippf[Se]_2$ (dippf = 1,1'-bis(di-iso-propylphosphano)ferrocene),[81] $dchpf[Se]_2$ (dchpf = 1,1'-bis(dicyclohexylphosphano)ferrocene),[82] $dchpdppf[Se]_2$ [dchpdppf = 1-(dicyclohexylphosphano)-1'-(diphenylphosphano)ferrocene],[25] $dippdppf[Se]_2$ [dippdppf = 1-(diisopropylphosphano)-1'-(diphenylphosphano)ferrocene],[25] $dppdtbpf[Se]_2$ [dppdtbpf = 1-(diphenylphosphano)-1'-(di-tert-butylphosphano)ferrocene][25] are reported in the literature, they were measured in $CDCl_3$ and therefore, could not be considered for this comparison.

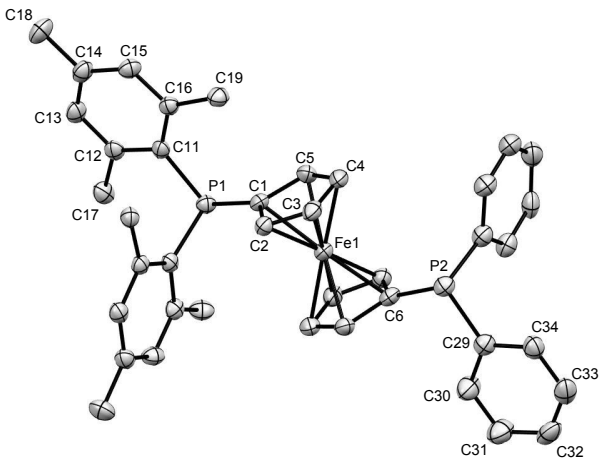

Fig 2. Ortep plots of the molecular structures of **3** in the solid state with ellipsoids drawn at the 50% probability level. Labels for some selected C atoms, solvent molecules and H atoms are omitted for clarity. Selected bond lengths [Å] and angles [°]: C(1)-C(2) 1.428(5), C(1)-P(1) 1.816(3), C(11)-P(1) 1.850(3), C(11)-C(16) 1.418(5), C(15)-C(16) 1.391(5), C(14)-C(15) 1.382(5), C(16)-C(19) 1.504(5), C(6)-P(2) 1.823(3), C(29)-P(2) 1.835(4), C(29)-C(34) 1.394(5), C(33)-C(34) 1.384(5), C(32)-C(33) 1.372(6), C(5)-C(1)-P(1) 122.7(3), C(1)-P(1)-C(11) 108.70(15), P(1)-C(11)-C(16) 127.6(2), C(6)-P(2)-C(29) 101.70(15).

Suitable single crystals for X-ray analyses were obtained for compounds **3**-**6**. While Figure 2 and 3 show the molecular structures of **3** and **5** respectively, their refinement data have been listed in Table S1 (SI file). The molecular structure of **3** in the solid state shows a sum of angles of 311.98(15)° at the phosphorus atom of the $PMes_2$ unit which is larger than the respective value for the PPh_2 unit in the same molecule (303.37(16)°), indicating increased steric interaction in the former.

Similar trends are found for **5** and **6** which are the selenophosphorane derivates of **1** and **3**. The sum of the C-P-C angles in **5** carrying two $PSeMes_2$ units is 319.5(1)° which is almost identical to the corresponding value of the $PSeMes_2$ unit in mixed substituted **6** (321.8(3)°), while the $PSePh_2$ unit shows only 315.2(2)°. Consistent with these findings the P-Se bond lengths are slightly longer in the sterically more demanding $PSeMes_2$ units (**5**: 2.1216(6) Å, **6**: 2.1246(14) Å) than in the $PSePh_2$ unit (**6**: 2.0971(13) Å). These structural features indicate a more pronounced dative P-Se interaction for the PPh_2 than for the $PMes_2$ unit in agreement with the NMR data outlined above, where the sterically less hindered phosphane unit entails larger $^1J_{P\text{-}Se}$ coupling values and stronger shielding of the ^{77}Se resonance in the corresponding selenophosphorane. The solid-state structures of **4** and **6** have been included in the SI file (Figures S65 and S66).

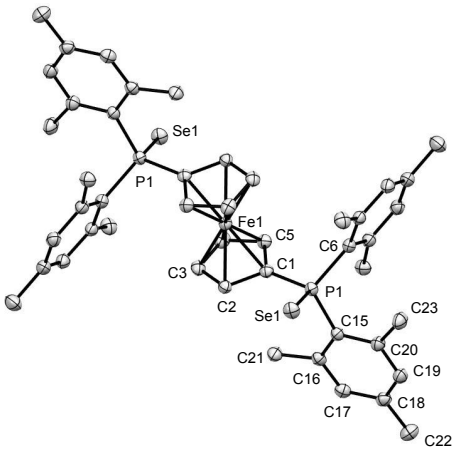

Fig 3. Ortep plots of the molecular structures of **5** in the solid state with ellipsoids drawn at the 50% probability level. Labels for some selected C atoms, solvent molecules and H atoms are omitted for clarity. Selected bond lengths [Å] and angles [°]: P(1)-C(1) 1.798(2), P(1)-Se(1) 2.1216(6), P(1)-C(6) 1.847(2), C(15)-C(20) 1.411(3), C(20)-C(23) 1.507(3), C(1)-C(5) 1.440(3), C(1)-Fe(1) 2.051(2), C(1)-P(1)-Se(1) 109.11(7), C(1)-P(1)-C(6) 102.94(10), C(1)-P(1)-C(15) 112.25(10), C(1)-P(1)-C(15) 112.25(10), C(6)-P(1)-Se(1) 122.09(7), C(15)-P(1)-Se(1) 106.20(7).

To explore the overall electronic effect of replacing phenyl with mesityl units in this molecular scaffold, the redox properties of the metallocene unit have been investigated using cyclic voltammetry (CV). The results, obtained by CV investigation, were further clarified by DFT calculations using ω-B97XD/6-311+G** level of theory (more details in SI file) as the oxidation of P(III) substituted ferrocenes may involve iron or phosphorus centred redox events.[83-89] Oxidation of compounds **1** and **3** occur at 0.13 V and 0.16 V (see Figures S69 and S70 in SI file), respectively, which are slightly shifted to lower potential in comparison to that of dppf (E° = 0.18 V). Investigating the Kohn-Sham molecular orbitals of **1**, **3** and the parent dppf, it could be established that the lone pairs of the phosphorus atoms have significant contribution to the HOMO (Figure 4; Figures S71 and S72 in SI file). In agreement with the increased bond angles around the phosphorus in case of $PMes_2$ units, the energy of this lone pair increases, thus it has more contribution to the HOMOs as well. It was in full agreement with the slightly shifted oxidation potential of **1** and **3**. The calculated spin density distribution of the corresponding cations of **1** and **3** are extensively localised at the iron center (Figure S73 in SI), thus the iron centred redox process is reversible for compound **3** (Figure S70 in SI file) and quasi-reversible for compound **1** (Figure S69 in SI file). Moreover, for both complexes, several follow up oxidation processes can be found at higher anodic potentials, which are likely to involve PR_2 moieties, in agreement with the significant contribution of the phosphorus lone pairs to the HOMO of

the corresponding dicationic species. These follow up oxidations are non-reversible and show small anodic shifts during reduction. To further characterize our ligands NBO calculations were performed, which reveal that changing the two phenyls to two mesityl groups, the p-character of the phosphorus lone pairs increased from 53% for dppf to 55-56% for **1** and **3** (Table S4 in SI file). Recently it was shown that the electronic effects of phosphorus containing bidentate ligands can be described by calculating the CO-stretching frequencies of corresponding L_2PdCO complexes (analogously to the experimental Tolman parameter).[43] This method (more details in SI file) has further been used to show that the electron donating ability increases from dppf to **1** and **3** in an order of dppf < **3** < **1** (Table S4 in SI file).

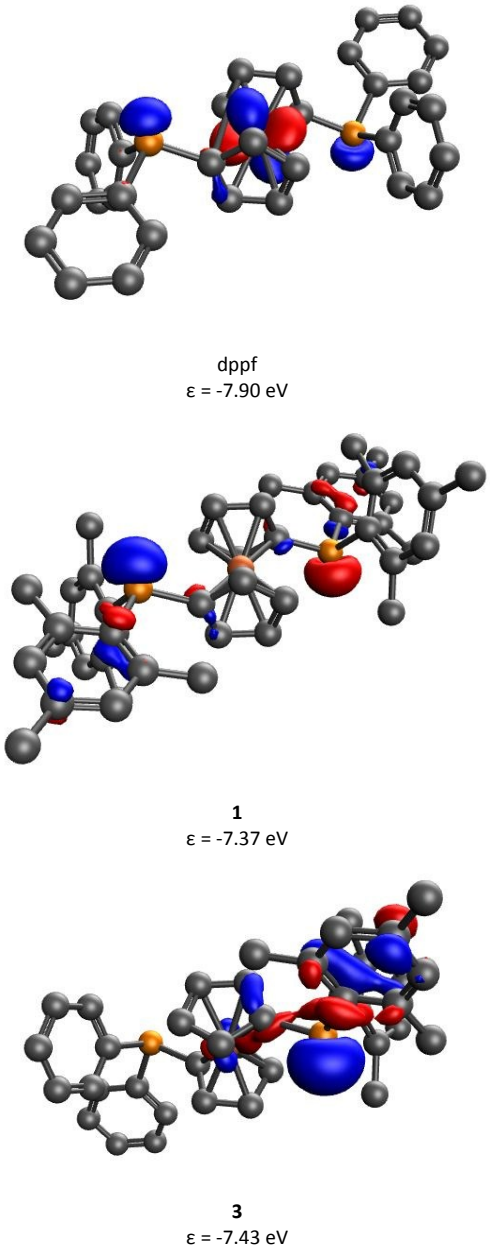

Fig. 4. The Kohn-Sham HOMOs of dppf, **1** and **3** (Structures were optimized at ω-B97XD/6-311+G** level of theory**).** Hydrogen atoms are omitted for clarity.

The previous findings classify **1** and **3** as electron rich ligand systems with increased steric congestion along with increased p-character of the phosphorus lone pair for the $PMes_2$ unit. To explore their ligand properties towards d-block metals and possible effects on catalytic systems Cu(I) complexes have been chosen, owing to their proclivity to adopt small coordination numbers for which steric effects should be less decisive. Using a common synthetic methodology CuX-complexes **7**-**12** (X = Br, I, $(MeCN)_nBF_4$, Chart 1) were synthesized from ligands **1** and **3**. Among them, the solid state structures could only be obtained for complex **10** and **12**, which are depicted in Figures 5 and 6, respectively. Although no suitable single crystals for X-ray analysis could be isolated for complexes **7**-**9**, their formation was indicated by the upfield shifts of ^{31}P signals (from δ -33.5 for **1** to δ -26.8 for **7**, δ -25.0 for **8** and δ -27.8 for **9**; see Figures S8, S28, S31 and S34 in SI file). Moreover, the broad lines in their ^{1}H and ^{31}P NMRs (see Figures S26-S34 in SI file) are suggesting a fast exchange of Cu^+ ions in the solution. On the other hand, the formation of complex **11** could be confirmed by the shifts and multiplicities of its ^{31}P signals [from δ -35.1 (s), -17.2 (s) for **3** to δ -30.1 (brm), -20.2 (d) for **11**, see Figures S17 and S45 in SI file], which suggest a coupling between two non-equivalent phosphorus atoms. It is needless to say that the evidence of similar P-P coupling could also be noticed for complexes **10** and **12** (see Figures S42 and S48 in SI file).

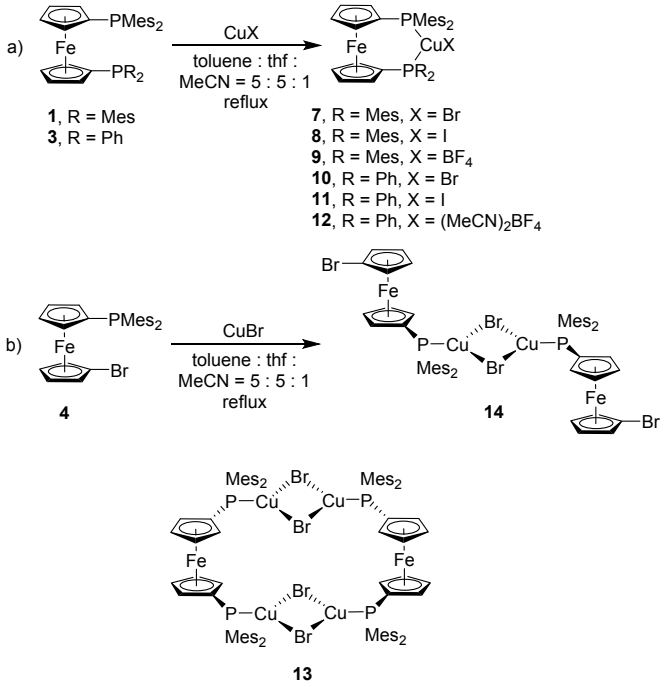

Scheme 5. CuX-complexes (X = Br, I, $(MeCN)_nBF_4$) of **1**, **3** and **4**.

The X-ray crystal structure of **10** and **12** revealed that the copper atoms are bonded to two phosphorus units with bite angles 116.53(6)° and 114.65(3)°, respectively (see Figures 5 and 6). As the mesityl group is bulkier than phenyl, the Cu-P bond in $P(Mes)_2$ side [2.2651(15) Å for **10** and 2.3302(8) Å for **12**] is slightly longer (1 pm for **10** and 9 pm for **12**) than the similar bond in PPh_2 side [2.2540(15) Å for **10** and 2.2437(8) Å for **12**], which introduces lower symmetry in complexes **10**-**12** for what a certain hemilability may be anticipated. To the best of our knowledge, there are only two complexes reported in the literature in which the ligands show a larger bite angle than **10** and both of them are based on dtbpf.[20, 51, 90] For comparison, a few related complexes, ordered by increasing

bite angles (in parentheses) are listed in the following: $[Cu_2(\mu\text{-}SCN)_2(\kappa^2\text{-}P,P\text{-}dppf)_2]$ (112.13(4)°),[20, 91] $[Cu_2(\mu_2\text{-}SCN)_2(\kappa^2\text{-}P,P\text{-}dppdtbpf)_2]$ (112.82(3)°),[90] $[Cu_2(\mu\text{-}CN)_2(\kappa^2\text{-}P,P\text{-}dppf)_2]$ (115.85(3)°),[92] $[Cu(\kappa^2\text{-}P,P\text{-}dppdtbpf)(CH_3CN)_2]PF_6$ (116.36(8)°),[90] $[Cu_2(\mu\text{-}NO_3\text{-}O)_2(\kappa^2\text{-}P,P\text{-}dppf)_2]$ (117.8(1)°),[93] [CuI(dtbpf)] (120.070(19))°.[51]

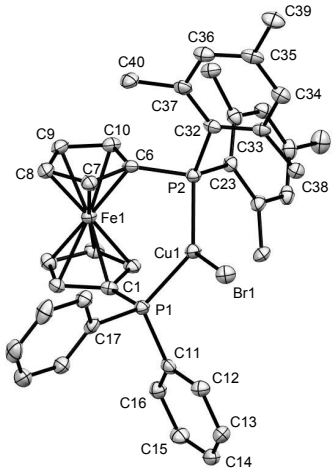

Fig 5. Ortep plots of the molecular structures of **10** in the solid state with ellipsoids drawn at the 50% probability level. Labels for some selected C atoms, solvent molecules and H atoms are omitted for clarity. The refinement data for this structure can be found in table S2 (SI file). Selected bond lengths [Å] and angles [°]: C(1)-P(1) 1.816(5), C(11)-P(1) 1.827(5), Cu(1)-P(1) 2.2540(15), Cu(1)-Br(1) 2.3428(9), Cu(1)-P(2) 2.2651(15), C(23)-P(2) 1.843(5), C(6)-P(2) 1.820(6), C(6)-P(2)-C(23) 103.7(2), C(23)-P(2)-C(32) 104.0(2), C(23)-P(2)-Cu(1) 120.25(17), C(32)-P(2)-Cu(1) 112.91(17), C(6)-P(2)-Cu(1) 104.52(17), C(6)-P(2)-C(32) 111.0(2), C(1)-P(1)-Cu(1) 115.88(17), C(1)-P(1)-C(11) 103.4(2), C(1)-P(1)-C(17) 102.4(2), C(11)-P(1)-Cu(1) 116.86(17), C(11)-P(1)-C(17) 102.4(2), P(1)-Cu(1)-Br(1) 113.81(5), P(2)-Cu(1)-Br(1) 128.24(5), P(1)-Cu(1)-P(2) 116.53(6).

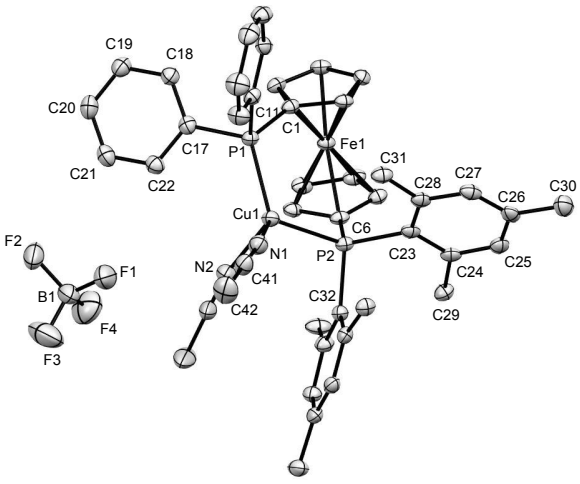

Fig 6. Ortep plots of the molecular structures of **12** in the solid state with ellipsoids drawn at the 50% probability level. When 50% split layer of acetonitrile has been shown, labels for some selected C atoms, other solvent molecules and H atoms are omitted for clarity. The refinement data for this structure can be found in table S2 (SI file). Selected bond lengths [Å] and angles [°]: C(1)-P(1) 1.803(3), C(11)-P(1) 1.829(3), Cu(1)-P(1) 2.2437(8), Cu(1)-P(2) 2.3302(8), C(6)-P(2) 1.818(3), C(23)-P(2) 1.853(3), Cu(1)-N(1) 2.018(3), C(6)-P(2)-Cu(1) 103.33(10), C(6)-P(2)-C(23) 103.77(13), C(32)-P(2)-C(23) 104.36(13), C(6)-P(2)-C(32) 112.34(13), C(32)-P(2)-Cu(1) 103.22(9), C(1)-P(1)-Cu(1) 113.69(10), C(1)-P(1)-C(11) 102.41(13), C(1)-P(1)-C(17) 103.13(14), C(17)-P(1)-Cu(1) 117.22(10), P(1)-Cu(1)-P(2) 114.65(3), N(1)-Cu(1)-N(2) 91.98(12), P(1)-Cu(1)-N(1) 115.34(8), P(1)-Cu(1)-N(2) 118.70(9), F(1)-B(1)-F(2) 108.9(3), F(1)-B(1)-F(4) 112.5(4), F(2)-B(1)-F(3) 110.3(4).

View Article Online
DOI: 10.1039/D0DT00941E

Upon recrystallization of complex **7**, crystals of complex **13** formed (see Scheme 5), along with micro-crystalline and powdery by-products. The X-ray crystal-structure of complex **13** shows a combination of 'double-bridge' and 'quasi-closed bridge' modes of coordination,[15] where two molecules of ligand **1** are connected via two diamond shaped (Cu_2Br_2) units (Figure 7). In order to avoid the formation of complex **13**, several steps have been taken, such as, changing the condition of crystallization and reaction of **1** with sub-stoichiometric amounts of CuBr (**1**: CuBr = 1: 0.8, 1: 0.7 and 1: 0.5). However, all these experiments resulted in complex **13** as the only crystalline product and **13** can be prepared in straightforward manner using the proper stoichiometry of metal to ligand.

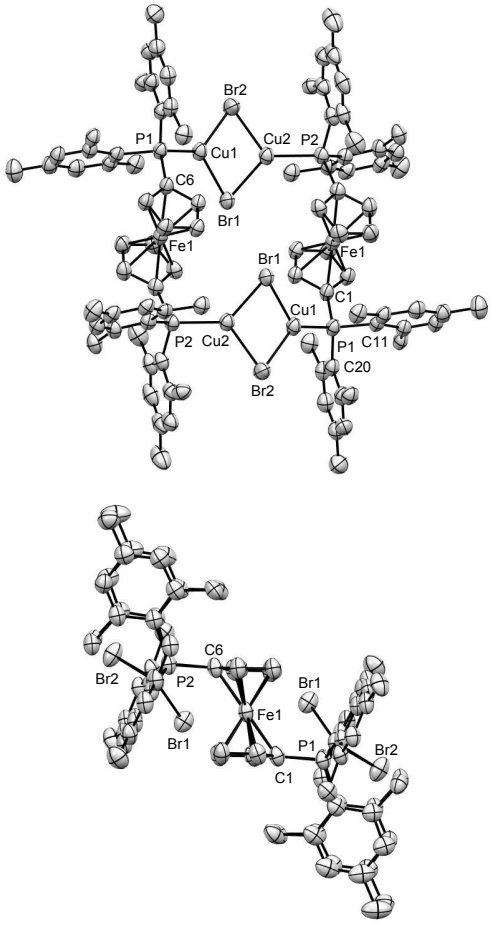

Fig 7. Ortep plot of the molecular structure of **13** in the solid state with ellipsoids drawn at the 50% probability level. Labels for some selected C atoms, solvent molecules and H atoms are omitted for clarity. When the figure at the top is showing the $[Cu_2Br_2]$ bridges, the figure at the bottom is showing the side view of the molecule. The plane of symmetry, passing through the four Br atoms, made this molecule achiral. The refinement data for this structure can be found in table S2, SI file. Selected bond lengths [Å] and angles [°]: C(1)-P(1) 1.804(6), C(11)-P(1) 1.831(6), Cu(1)-P(1) 2.2095(16), Cu(2)-P(2) 2.2059(15), Cu(1)-Br(1) 2.3949(10), Cu(1)-Cu(2) 2.9295(11), C(1)-P(1)-C(11) 102.7(3), C(1)-P(1)-C(20) 110.4(3), C(1)-P(1)-Cu(1) 110.21(19), Cu(1)-P(1)-C(11) 121.37(19), Cu(1)-P(1)-C(20) 103.6(2), C(20)-P(1)-C(11) 108.5(3), P(1)-Cu(1)-Br(1) 131.98(5), P(1)-Cu(1)-Br(2) 124.84(5), Br(1)-Cu(1)-Br(2) 102.34(4), Cu(1)-Br(1)-Cu(2) 74.46(3), Cu(2)-Cu(1)-Br(1) 53.57(3).

The complexation via the formation of Cu_2X_2 (X = Cl, Br, I) bridges is common for dppf,[51, 92-96] and some sterically encumbered dppf analogs.[90, 97-99] However, apart from this rare bonding motif, the classical chelating coordination mode of single metal centre is also known for them.[25, 90, 100] For the [Mes_2P]-substituted ferrocene ligands, the formation of Cu_2X_2 bridges seems to be favoured as non-chelating ligand **4** similarly results in this motif to complex **14**, which was synthesized by reacting **4** with one equivalent of CuBr. X-ray crystallographic analysis revealed that this complex shows a similar bonding motif as **13**, where two molecules of **4** are bridged by one planar Cu_2Br_2 unit (Figure 8). The distances between the Cu atoms in the Cu_2Br_2 moieties of complex **13** and **14** are ca. 2.93 and 3.07 Å, respectively. These values are significantly lower, compared to the similar Cu-Cu distances of other halogen-bridged complexes, reported in the literature.[92, 94-96]

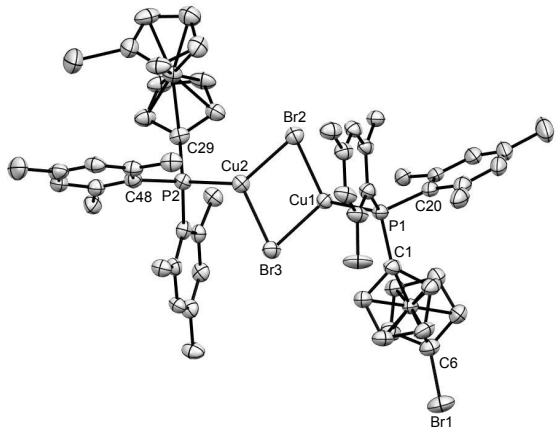

Fig 8. Ortep plot of the molecular structure of **14** in the solid state with ellipsoids drawn at the 50% probability level. Labels for some selected C atoms, solvent molecules and H atoms are omitted for clarity. While the refinement data for this structure is listed in Table S2 (SI file) the side view of this molecule is shown in Figure S67 (SI file). The refinement data for this structure can be found in table S2, SI file. Selected bond lengths [Å] and angles [°]: C(1)-P(1) 1.815(6), C(20)-P(1) 1.842(6), Cu(1)-P(1) 2.2044(15), Cu(1)-Br(2) 2.4592(9), Br(1)-C(6) 1.886(6), C(1)-P(1)-Cu(1) 111.33(18), C(1)-P(1)-C(20) 102.1(3), C(1)-P(1)-Cu(1) 111.33(18), Cu(1)-P(1)-C(20) 121.7(2), P(1)-Cu(1)-Br(2) 130.81(5), P(1)-Cu(1)-Br(3) 127.82(5), Cu(1)-Br(2)-Cu(2) 78.64(3).

Catalysis

Complexes **7**-**12** were then used to explore their catalytic activity in the CO_2-fixation of terminal alkynes as outlined in the introduction. In this investigation, the carboxylation of phenylacetylene was selected as a model reaction to study the influence of various ligands on catalysis compared with CuI, CuBr and $Cu(MeCN)_4BF_4$.

As shown in Figure 9, complexes **7**-**12** exhibited higher catalytic activity compared to the free copper salts. The maximum increase of such catalytic activity can be seen for the $Cu(MeCN)_nBF_4$ analogs, where the yield increased from 29% for $Cu(MeCN)_4BF_4$, to 59% and 76% for complexes **9** and **12** respectively (Entries 3, 6, and 9, Table 1; Figure 9). However, the catalytic advantage of such complexes over the simple Cu halide decreases as the size of the halide increases [CuBr salts: 41% for CuBr, to 62% for **7**, and 88% for **10** (Entries 2, 4 and 7, Table 1; Figure 9); CuI salts: 58% for CuI to 69% for **8** and 86% for **11** (Entries 1, 5 and 8, Table 1; Figure 9)]. In order to draw a fair comparison between dppf and our ligands (i.e. **1** and **3**), similar catalytic reaction was further carried out with dppf·$Cu(MeCN)_2BF_4$ (Entry 10, Table 1) as a catalyst, where 33% yield have been obtained, which was slightly higher than free $Cu(MeCN)_4BF_4$, but significantly lower than **9** and **12** (Entries 6 and 9, Table 1). For the sake of completeness, it should be mentioned that CuCl and its respective complexes were not included into this comparison as they showed much lower catalytic conversion (ca. 5-10%) at otherwise identical conditions with no significant difference between complexes and free salt.

Table 1. Survey of catalytic activity in the formation of phenylpropiolic acid from phenylacetylene using 3 mol% of the respective catalysts (cf. table S3 further details and variations).

Entry	Catalyst	Product yield
1	CuI	58
2	CuBr	41
3	$Cu(MeCN)_4(BF_4)$	29
4	**7**	62
5	**8**	69
6	**9**	59
7	**10**	88
8	**11**	86
9	**12**	76
10	dppf·$Cu(MeCN)_2(BF_4)$	33

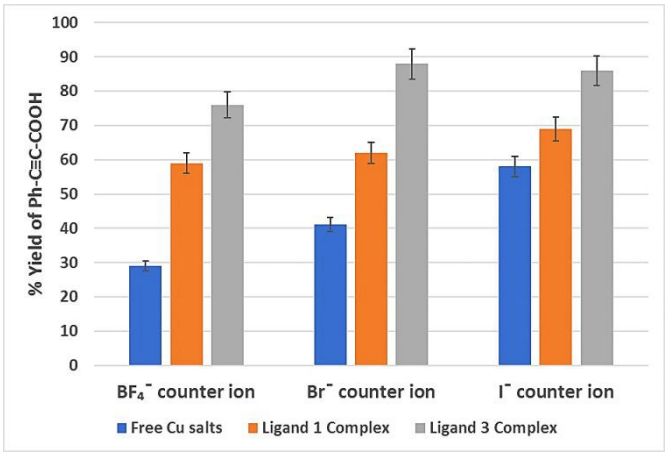

Fig 9. Catalytic efficiency for the carboxylation reaction from Ph-C≡CH to Ph-C≡C-COOH. The blue, orange and grey bars show the yields resulting from free copper salts, corresponding Cu(I) complexes with ligand **1** and **3**, respectively. As the yields listed here are the averages of two consecutive catalytic reactions, error bars of 5% are shown for all yields.

In general, the catalytic activity of complexes of phosphane ligands is raised by increasing the steric bulk of the substituents on phosphorus.[21, 51] An opposite trend is being noticed in our case, where complexes **10**-**12** produce higher yields than **7**-**9** (Table S3, SI file) which may be attributed to the complexation mode observed for ferrocene based ligands where all phosphorus donor sites are mesityl substituted. Complexes **13** and **14** are the only examples for these ligands where structural information is available and show this feature consistently. Since the conversion of **7** to **13** involves the transfer of CuBr units, it can be speculated that in complexes **7**-**9** the metal is more loosely bound, due to the high steric bulk of ligand **1**.

The lower complex stability of Cu(I) with **1** (in comparison to **3**) was further corroborated by the **7**+**3**→**10**+**1** ligand-exchange reaction, which is slightly exothermic (-4.4 kcal/mol at the ω-B97X-D/6-311+G**//ω-B97X-D/6-31G* level of theory, Figure S74 in SI file). To test this hypothesis experimentally, the organic washings of the catalytic reactions were collected, dried under high vacuum, and analyzed by ^{31}P NMR, which revealed that complexes **7**-**9** dissociate to give free ligand **1** during catalysis (Figures S55 and S56 in SI file), whereas for complexes **10**-**12** the Cu-P bonds remain intact (Figures S57 and S58 in SI file). It should be highlighted that we have further investigated computationally the CO_2 insertion step in the catalytic system, which is usually the rate limiting step.[101, 102] The calculated reaction barriers are somewhat lower (by 1.2 kcal/mol at the ω-B97X-D/6-311+G**//ω-B97X-D/6-31G* level of theory) in case of the complexes with **3** in comparison to those of **1**, which can be also an explanation for the lower activity of its complexes (see Table S5 in the SI file).

Conclusion

In summary, the tetra- and dimesityl analogs of dppf, **1** and **3**, have been synthesized and their ligand properties were explored. The phosphorus lone pairs of tetramesityl substituted **1** show lower *s* character, and therefore, higher donating ability than those in Ph_3P and dppf as indicated by spectroscopic, structural, electrochemical and computational means. In line with these experimental findings the lone pair at phosphorus makes a significant contribution to the HOMO in **1** and **3**, which explains the cathodic shift of the oxidation potentials with increasing mesityl substitution. For a series of Cu(I) complexes of these ligands a variety of structural motifs has been found, ranging from the rare double bridging mode over dimeric bridging to isolated Cu-centers. With unsymmetrical ligand **3** stable complexes were formed with isolated Cu(I) centers, while the sterically more challenged tetramesityl substituted **1** is prone to dimeric bridging with increased separation of the phosphorus atoms and its adjacent mesityl substituents. As a consequence of its hemilabile nature, the Cu(I) complexes of **3** showed improved catalytic activity in the addition of CO_2 to terminal alkynes as compared with the respective complexes of **1** which in turn performed superior to the respective dppf complexes. The potential of these ligands for complexation of other metals and the catalytic activity of these complexes will be explored in the near future.

Experimental Section

All manipulations were performed under Argon atmosphere unless mentioned otherwise. Prior to use, the glasswares were dried in drying oven under 120 °C. Solvents were distilled over drying agents, prescribed in CRC Handbook of chemistry and subsequently stored under Argon atmosphere over 4 Å molecular sieves. Solvents for column chromatography and aqueous workups were used from bottle (analytical grade supplied by VWR and Alfa-Aesar) without further purification. NMR solvents (purchased from Deutero) were degassed via a few cycles of freeze, pump and thaw, and finally stored over 3 Å molecular sieves under Argon atmosphere.

Reagents and chemicals were purchased from commercial suppliers (Sigma-Aldrich, ABCR, Alfa-Aesar) and used as received. Fc'$(PCl_2)_2$, MesLi·LiBr·OEt_2 and dppf·Cu$(MeCN)_2BF_4$ were synthesized by following the procedure, reported in the literature.[56, 57, 103, 104] Mes_2PX (X = Cl/Br, 48%/52%; Figures S1 and S2 in SI file) was synthesized by following the procedure, reported for Xyl_2PX (X = Cl, Br).[105] It should be noted that all the chemical manipulations involving Mes_2PX as a reagent, require careful calculations of its formula weights. This is because, the ^{1}H NMR spectra of Mes_2PX, obtained from different preparation attempts, have shown different proportional ratios of Mes_2PCl and Mes_2PBr (e.g. 48:52 and 53:47). Due to minor side reactions, such as, unwanted dilithiation and subsequent in situ hydrolysis, compounds **3** and **4** contain an impurity, where only dimesitylphosphano group is present on ferrocene. We could not remove this compound from the targeted species and, therefore, used species **3** and **4**, contaminated with ca. 1-4% of dimesitylphosphanoferrocene for the next chemical transformations (see Figure S9, S12 and S13 in SI file).

NMR spectra were measured with Varian 500VNMRS and Varian MR-400 spectrometers at 22 °C. Chemical shifts (δ in ppm) were expressed with respect to the following standards, set as 0 ppm: $SiMe_4$ (for ^{1}H and ^{13}C), aqueous H_3PO_4 (for ^{31}P), $BF_3{\cdot}OEt_2$ (in $CDCl_3$ for ^{11}B) and $CFCl_3$ (for ^{19}F). The peaks, resulting from the residual non-deuterated NMR solvents, were locked as indicated in the literature.[106] In addition to the standard notation of the signal multiplicity (s = singlet, d = doublet, m = multiplet, dd = doublet of doublet etc.), pst, brs, brd and brm were used to abbreviate pseudo-triplet, broad singlet, broad doublet and broad multiplet, respectively in order. The amount of residual solvents (if present) was verified by NMR analysis and the expected values for elemental analyses were calculated accordingly. When the NMRs of compounds **1** and **3**-**6** were measured in toluene-d8 and thf-d8, those for the corresponding complexes (**7**-**12**, **14**) were only measured either in thf-d8 or CD_3CN. This is because, the complexes could not be dissolved in toluene-d8 by any means. Due to the reason of lower solubility even in the donating solvents (like thf-d8 or CD_3CN), the ^{13}C NMRs of some complexes are relatively poor and as a result, signals for the ipso-carbons could not be seen after substantially high number of scans. On the other hand, the diphosphano ferrocene ligands were insoluble in CD_3CN and therefore, the NMRs in the corresponding solvent could not be measured.

Infrared spectra measured from the neat substances of **9** and **12** were obtained by a Bruker Alpha Platinum ATR spectrometer, where opus 6.5 (by Bruker Optics) was used for analysing the data. Strong, medium strong and week peaks for these species have been denoted as s, m and w, respectively. For the sake of comparison, Infrared spectra of Cu$(MeCN)_4BF_4$ and dppf·Cu$(MeCN)_2BF_4$ were also measured under identical conditions for comparison and have been depicted in SI file (Figure S75). When Electrospray ionisation (ESI) and Atmospheric pressure chemical ionization (APCI) mass spectra were measured with a Finnigan LCQ Deca (ThermoQuest, San Jose, USA) instrument using samples dissolved in HPLC-quality thf, MALDI was measured with an UltraFlex ToF / ToF (Bruker Daltonics, Bremen, D) instrument, where an N2 laser with 337 nm wavelength and 3 ns pulse duration was used. The matrix used for MALDI measurements was DCTB (2-[(2E)-3-(4-tert-butylphenyl)-2-methylprop-2-enylidene] malononitrile). Elemental analyses were performed without the presence of any external oxidizer (like V_2O_5) in an EA 3000 Elemental Analyzer (EuroVector). X-ray diffraction experiments were performed using either a STOE IPDS II [using Mo-Kα source (λ = 0.71073 Å)] or a STOE StadiVari [using either Mo-GENIX source (λ = 0.71073 Å), or Cu-GENIX source (λ = 1.54186 Å)] diffractometer. Structures were solved using dual space method (SHELXT) and were refined with SHELXL-2018.[107] All non-hydrogen atoms were refined anisotropically, whereas hydrogen atoms were placed on adjacent

atoms using a riding model. Further programs used in the structure analyses were Mercury and Platon.[108-110]

All cyclic voltammetry measurements were carried out in an MBraun acrylic glovebox GB2202-C-VAC under Argon atmosphere. Samples were measured as a solution (0.1 M) in dry and deoxygenated CH_2Cl_2, where anhydrous $[Bu_4N][PF_6]$ was used as conducting salt at a concentration of 0.1 M. The three-electrode cell consisted of a platinum working electrode, a silver counter electrode and a silver pseudo reference electrode. The potential was driven on a WaveDriver 20 Bipotentiostat from Pine Research Instrument and the electrochemical data was recorded via AfterMath (Ver. 1.5.9807, Pine Instrument). All the redox processes were refenced using half wave potentials of $(C_5Me_5)_2Fe$ as standard, which was added to the analyzed solution. Its corresponding value was then subtracted from the recorded potentials to convert them to the Fc/Fc^+ scale following established procedures,[111] and finally evaluated with AfterMath and Excel.

Fc'(PMes$_2$)$_2$ (1). A solution of Fc'$(PCl_2)_2$ (0.388 g, 1.00 mmol) in thf (10 mL) was added dropwise to a cold (-84 °C) and stirred suspension of MesLi·LiBr·OEt_2 (1.145 g, 3.99 mmol) in hexanes (100 mL). The reaction mixture was slowly warmed to rt over 3-4 hrs and stirred for 18 hrs at rt. After all the volatiles were removed under vacuum (10^{-3} mbar), the resulting compound was extracted in toluene (60 mL) and tested with ^{7}Li NMR. A small peak at δ 7.33 ppm in ^{7}Li NMR indicated the presence of soluble LiCl in the crude, which was further evacuated to dryness and extracted with toluene (30 mL). The volume of thus obtained toluene solution was reduced to c.a. 5 mL and finally precipitated on cold (-20 °C) and vigorously stirred mixture of Et_2O and pentane (40 mL, 1:1). The supernatant solution was carefully decanted and the precipitate was dried under high vacuum (10^{-3} mbar), resulting in compound **1** as a pale yellow amorphous solid (70%). **NOTE** This compound have also been synthesized (with a yield of 66%) by the reaction of $FcLi_2\cdot(tmeda)_{2/3}$ (1 mmol) and Mes_2PX (X = Cl/Br, 48%/52%, FW = 327.914 g/mol, 0.669 g, 2.04 mmol) in thf at -84 °C, with a subsequent workup as mentioned above. ^{1}H NMR (toluene-d8): δ 2.08 (s, 12H, *p*-CH_3 of Mes), 2.31 (s, 24H, *o*-CH_3 of Mes), 4.20 (m, 4H, β-H of Cp), 4.25 (m, 4H, α-H of Cp), 6.66 (brs, 8H, *m*-H of Mes). ^{1}H NMR (thf-d8): δ 2.17 (s, 24H, *o*-CH_3 of Mes), 2.18 (s, 12H, *p*-CH_3 of Mes), 4.19 (m, 4H, β-H of Cp), 4.22 (m, 4H, α-H of Cp), 6.74 (brs, 8H, *m*-H of Mes). $^{13}C\{^1H\}$ NMR (toluene-d8): δ 21.28 (s, *p*-CH_3 of Mes), 23.47 (d, *o*-CH_3 of Mes, *J* = 15 Hz), 72.50 (d, β-C of Cp, *J* = 4 Hz), 76.00 (d, α-C of Cp, *J* = 19 Hz), 80.14 (d, ipso-C of Cp, *J* = 13 Hz), 127.34 (s, *p*-Aryl *C* of Mes), 130.48 (d, *m*-Aryl *C* of Mes, *J* = 3 Hz), 132.65 (d, *ipso*-Aryl *C* of Mes, *J* = 21 Hz), 142.53 (d, *o*-Aryl *C* of Mes, *J* = 15 Hz). $^{13}C\{^1H\}$ NMR (thf-d8): δ 20.72 (s, *p*-CH_3 of Mes), 23.29 (d, *o*-CH_3 of Mes, *J* = 15 Hz), 72.68 (d, β-C of Cp, *J* = 4 Hz), 76.24 (d, α-C of Cp, *J* = 18 Hz), 80.27 (d, ipso-C of Cp, *J* = 13 Hz), 130.52 (d, *p*-Aryl *C* of Mes, *J* = 4 Hz), 132.82 (d, *ipso*-Aryl *C* of Mes, *J* = 20 Hz), 137.95 (s, *m*-Aryl *C* of Mes), 142.75 (d, *o*-Aryl *C* of Mes, *J* = 15 Hz). $^{31}P\{^1H\}$ NMR (toluene-d8): δ -35.1. $^{31}P\{^1H\}$ NMR (thf-d8): δ -33.5. MS (APCI-DIP): m/z (%) 722 (100) $[M]^+$. HRMS (APCI-DIP; m/z): $[M]^+$ calc for $C_{46}H_{52}FeP_2$, 722.28937; found 722.28882. Anal. Calcd. for $C_{46}H_{52}FeP_2$: C, 76.45; H, 7.25. Found: C 75.23; H, 7.16. Probably due to the presence of a little amount of LiCl, the CHN values for this compound differ significantly than expected. As these values could not be improved after several attempts, the purity of the species was further clarified by mass spectrometry (see Figure S68 in SI file).

Fc'(PMes$_2$)Br (4). ^{n}BuLi (2.5 M in hexanes, 0.84 mL, 2.10 mmol) was added dropwise to a cold (-84 °C) and stirred thf (20 mL) solution of dibromoferrocene (0.687 g, 2.00 mmol). After the gradual color change from pale yellow to bright orange, the solution was stirred at -84 °C for another 30 mins. Another solution of Mes_2PX (X = Cl/Br, 48%/52%, FW = 327.914 g/mol, 0.679 g, 2.07 mmol) in thf (20 mL) was slowly added to the previous cold solution over 5 mins. After warming up to the ambient temperature, the reaction mixture was stirred for overnight. All the volatiles were removed under high vacuum (10^{-3} mbar) and the product was extracted with hexanes (50 mL). The volume of the filtrate was reduced to ca. 10mL and the almost pure compound was obtained as yellow crystals upon refrigeration at -78 °C. This product had an impurity of dimesitylphosphanoferrocene (ca. 5%) which could be reduced to ca. 2-3% upon further crystallization in hexanes at -10 °C and the final product was obtained as bright orange crystals (53%). ^{1}H NMR (C_6D_6): δ 2.08 (s, 6H, *p*-CH_3 of Mes), 2.37 (s, 12H, *o*-CH_3 of Mes), 3.85 (pst, 2H, β-H of Cp^{Br}), 4.19 (pst, 2H, α-H of Cp^{Br}), 4.23 (pst, 2H, β-H of Cp^{PMes2}), 4.32 (m, 2H, α-H of Cp^{PMes2}), 6.71 (d, 4H, *m*-H of Mes, *J* = 3 Hz). $^{13}C\{^1H\}$ NMR (C_6D_6): δ 20.89 (s, *p*-CH_3 of Mes), 23.51 (d, *o*-CH_3 of Mes, *J* = 15 Hz), 69.04 (s, β-C of Cp^{Br}), 71.59 (s, α-C of Cp^{Br}), 74.20 (d, β-C of Cp^{PMes2}, *J* = 4 Hz), 77.23 (d, α-C of Cp^{PMes2}, *J* = 18 Hz), 78.09 (s, ipso-C of Cp^{Br}), 81.55 (d, ipso-C of Cp^{PMes2}, *J* = 13 Hz), 130.57 (d, *m*-Aryl *C* of Mes, *J* = 3 Hz), 132.47 (d, *o*-Aryl *C* of Mes, *J* = 21 Hz), 137.81(s, *p*-Aryl *C* of Mes), 142.57 (d, *ipso*-Aryl *C* of Mes, *J* = 14 Hz). $^{31}P\{^1H\}$ NMR (C_6D_6): δ -35.5. MS (APCI-DIP): m/z (%) 533 (100) $[M]^+$. HRMS (APCI-DIP; m/z): $[M]^+$ calc for $C_{28}H_{30}BrFeP$, 533.06179; found 533.069069. Anal. Calcd. for $C_{28}H_{30}BrFeP$: C, 63.07; H, 5.67. Found: C, 63.32; H, 5.75.

Fc'(PMes$_2$)(PPh$_2$) (3). ^{n}BuLi (2.5 M in hexanes, 0.15 mL, 0.38 mmol) was added dropwise to a cold (0 °C) thf (20 mL) solution of Fc'$(PMes_2)$Br (0.200 g, 0.38 mmol). After the gradual color change from orange to bright red, the solution was stirred at 0 °C for 30 mins. Another solution of Ph_2PCl (72 μL, 0.086 g, 0.40 mmol) in hexanes (10 mL) was slowly added to the previous cold solution over 5 mins. After warming up to the ambient temperature, the reaction mixture was stirred overnight. All the volatiles were removed under high vacuum (10^{-3} mbar) and the product was extracted with hexanes (20 mL). The volume of the filtrate was reduced to ca. 5 mL and the almost pure compound was obtained as yellow crystals (62%) upon refrigeration at -78 °C. This product had an impurity of dimesitylphosphanoferrocene (ca. 3-4%) which could not be reduced upon further crystallization. ^{1}H NMR (toluene-d8): δ 2.08 (s, 6H, *p*-CH_3 of Mes), 2.30 (s, 12H, *o*-CH_3 of Mes), 4.04 (m, 2H, β-H of Cp^{PPh2}), 4.10 (pst, 2H, α-H of Cp^{PPh2}), 4.17 (m, 2H, β-H of Cp^{Mes}), 4.21 (pst, 2H, α-H of Cp^{Mes}), 6.66 (brd, 4H, *m*-H of Mes, *J* = 3 Hz), 7.01-7.02 (m, 6H, *m* and *p*-H of Ph), 7.38 (m, 4H, *o*-H of Ph). ^{1}H NMR (thf-d8): δ 2.16 (s, 12H, *o*-CH_3 of Mes), 2.19 (s, 6H, *p*-CH_3 of Mes), 4.01 (m, 2H, β-H of Cp^{PPh2}), 4.14 (m, 2H, α-H of Cp^{PPh2}), 4.18 (m, 2H, β-H of Cp^{Mes}), 4.26 (pst, 2H, α-H of Cp^{Mes}), 6.74 (brd, 4H, *m*-H of Mes, *J* = 3 Hz), 7.23-7.29 (m, 10H, *o*, *m* and *p*-H of Ph). $^{13}C\{^1H\}$ NMR (toluene-d8): δ 20.87 (s, *p*-CH_3 of Mes), 23.47 (d, *o*-CH_3 of Mes, *J* = 15 Hz), 72.27 (d, β-C of Cp^{PPh2}, *J* = 3 Hz), 72.80 (d, β-C of Cp^{PMes2}, *J* = 4 Hz), 74.28 (d, α-C of Cp^{PPh2}, *J* = 15 Hz), 75.86 (d, α-C of Cp^{PMes2}, *J* = 18 Hz), 77.34 (d, ipso-C of Cp^{PPh2}, *J* = 10 Hz), 80.57 (d, ipso-C of Cp^{PMes2}, *J* = 13 Hz), 128.34 (d, *m*-Aryl *C* of Ph, *J* = 7 Hz), 128.57 (s, *p*-Aryl *C* of Ph), 130.49 (d, *m*-Aryl *C* of Mes, *J* = 3 Hz), 132.61 (d, *o*-Aryl *C* of Mes, *J* = 21 Hz), 133.92 (d, *o*-Aryl *C* of Ph, *J* = 21 Hz), 140.05 (d, *ipso*-Aryl *C* of Ph, *J* = 15 Hz), 142.54 (d, *ipso*-Aryl *C* of Mes, *J* = 15 Hz). $^{13}C\{^1H\}$ NMR (thf-d8): δ 20.90 (s, *p*-CH_3 of Mes), 23.48 (d, *o*-CH_3 of Mes, *J* = 15 Hz), 72.68 (dd, β-C of Cp^{PPh2}, *J* = 4, 1 Hz), 73.11 (d, β-C of Cp^{PMes2}, *J* = 4 Hz), 74.63 (d, α-C of Cp^{PPh2}, *J* = 15 Hz), 76.28 (d, α-C of Cp^{PMes2}, *J* = 18 Hz), 77.71 (d, ipso-C of Cp^{PPh2}, *J* = 10 Hz), 80.81 (d, ipso-C of Cp^{PMes2}, *J* = 13 Hz), 128.78 (d,

m-Aryl *C* of Ph, *J* = 7 Hz), 129.09 (s, *p*-Aryl *C* of Ph), 130.70 (d, *m*-Aryl *C* of Mes, *J* = 3 Hz), 132.95 (d, *o*-Aryl *C* of Mes, *J* = 21 Hz), 134.27 (d, *o*-Aryl *C* of Ph, *J* = 20 Hz), 138.11 (s, *p*-Aryl *C* of Mes), 140.43 (d, *ipso*-Aryl *C* of Ph, *J* = 11 Hz), 142.91 (d, *ipso*-Aryl *C* of Mes, *J* = 15 Hz). $^{31}P\{^1H\}$ NMR (toluene-d8): δ -34.8 (*P*Mes$_2$), -17.0 (*P*Ph$_2$). $^{31}P\{^1H\}$ NMR (thf-d8): δ -35.1 (*P*Mes$_2$), -17.2 (*P*Ph$_2$). MS (APCI-DIP): m/z (%) 639 $[M+1]^+$. HRMS (APCI-DIP; m/z): $[M+1]^+$ calc for $C_{40}H_{40}FeP_2$, 639.19547; found 639.20281. Anal. Calcd. for $C_{40}H_{40}FeP_2$: C, 75.24; H, 6.31. Found: C, 74.92; H, 6.45.

Diselenide derivatives of 1 and 3. A suspension of red Se (0.120 g, 1.52 mmol) and **1** (0.170 g, 0.24 mmol) or **3** (0.153 g, 0.24 mmol) in thf (20 mL) was stirred for 1 hr at r.t. All the volatiles were removed under high vacuum (10^{-3} mbar) and the product was extracted with hot toluene. Analytically pure compound was crystallized from the hot toluene solution by slow cooling up to ambient temperature. **NOTE** If all the residual Se is not removed by single filtration attempt, the procedure of filtration must be repeated for multiple times before crystallization.

Fc'(PSeMes$_2$)$_2$ (5). Yield: 67%. ^{1}H NMR (toluene-d8): δ 1.99 (s, 12H, *p*-C*H*$_3$ of Mes), 2.38 (brs, 24H, *o*-C*H*$_3$ of Mes), 4.79 (m, 4H, Cp), 4.90 (brs, 4H, Cp), 6.52 (m, 8H, *m*-H of Mes). $^{13}C\{^1H\}$ NMR (toluene-d8): δ 24.43 (d, *o*-*C*H$_3$ of Mes, *J* = 6 Hz), 75.72 (d, β-C of Cp, *J* = 9 Hz), 78.25 (brs, α-C of Cp), 82.45 (d, ipso-C of Cp, *J* = 78 Hz), 125.63 (s, *p*-Aryl *C* of Mes), 132.15 (d, *o*-Aryl *C* of Mes, *J* = 11 Hz), 139.72 (d, *m*-Aryl *C* of Mes, *J* = 2 Hz), 140.49 (brm, *ipso*-Aryl *C* of Mes). $^{31}P\{^1H\}$ NMR (toluene-d8): δ 14.7 ($^1J_{P,Se}$ = 723 Hz). $^{77}Se\{^1H\}$ NMR (toluene-d8): δ -82.6 (P*Se*Mes$_2$, $^1J_{P,Se}$ = 723 Hz). MS (MALDI): m/z (%) 880 (100) $[M]^+$. Anal. Calcd. for $C_{46}H_{52}FeP_2Se_2$: C, 62.74; H, 5.95. Found: C, 62.89; H, 5.90.

Fc'(PSeMes$_2$)(PSePh$_2$) (6). Yield: 65%. ^{1}H NMR (toluene-d8): δ 1.99 (s, 6H, *p*-C*H*$_3$ of Mes), 2.35 (brs, 12H, *o*-C*H*$_3$ of Mes), 4.42 (brs, 2H, β-H of Cp^{PPh2}), 4.69 (brs, 2H, α-H of Cp^{PPh2}), 4.73 (brs, 2H, α-H of Cp^{Mes}), 4.76 (brs, 2H, β-H of Cp^{Mes}), 6.49 (brd, 4H, *m*-H of Mes, *J* = 4 Hz), 6.92-6.94 (m, 6H, *m* and *p*-H of Ph), 7.70 (m, 4H, *o*-H of Ph). $^{13}C\{^1H\}$ NMR (toluene-d8): δ 20.69 (d, *p*-*C*H$_3$ of Mes, *J* = 2 Hz), 24.32 (d, *o*-*C*H$_3$ of Mes, *J* = 6 Hz), 74.94 (d, β-C of Cp^{PPh2}, *J* = 12 Hz), 75.38 (d, α-C of Cp ^{PPh2}, *J* = 9 Hz), 75.99 (d, ipso-C of Cp^{PPh2}, *J* = 86 Hz), 76.12 (d, β-C of Cp^{PMes2}, *J* = 10 Hz), 78.05 (brd, α-C of Cp ^{PMes2}, *J* = 13 Hz), 82.82 (d, ipso-C of Cp^{PMes2}, *J* = 78 Hz), 128.27 (d, *p*-Aryl *C* of Ph, *J* = 3 Hz), 131.10 (d, *m*-Aryl *C* of Ph, *J* = 3 Hz), 132.08 (d, *o*-Aryl *C* of Ph, *J* = 11 Hz), 132.38 (d, *o*-Aryl *C* of Mes, *J* = 11 Hz), 134.34 (d, *ipso*-Aryl *C* of Ph, *J* = 78 Hz), 139.62 (d, *m*-Aryl *C* of Mes, *J* = 3 Hz), 140.39 (brd, *ipso*-Aryl *C* of Mes). $^{31}P\{^1H\}$ NMR (toluene-d8): δ 14.8 (*P*Mes$_2$, $^1J_{P,Se}$ = 723 Hz), 30.8 (*P*Ph$_2$, $^1J_{P,Se}$ = 763 Hz). $^{77}Se\{^1H\}$ NMR (toluene-d8): δ -298.8 (P*Se*Ph$_2$, $^1J_{P,Se}$ = 763 Hz), -77.5 (P*Se*Mes$_2$, $^1J_{P,Se}$ = 723 Hz). MS (ESI): m/z (%) 797 (100) $[M+1]^+$. HRMS (ESI; m/z): $[M+1]^+$ calc for $C_{40}H_{40}FeP_2Se_2$, 799.02851; found 799.03579. Anal. Calcd. for $C_{40}H_{40}FeP_2Se_2$: C, 60.32; H, 5.06. Found: C, 60.44; H, 5.17.

Copper complexes of 1. A suspension of **1** (0.144 g, 0.20 mmol), CuX (0.20 mmol), toluene (10 mL), thf (10 mL) and CH_3CN (2 mL) was refluxed for 24 hrs. After removal of all insoluble materials by filtration, the volume of the filtrate was reduced to ca. 15 mL and analytically pure crystalline or semi-crystalline materials were obtained by slow introduction of dry pentane while kept in a double arm H-tube at ambient temperature. For all the compounds, mentioned under this section, the mass spectrometric measurements gave similar data, where corresponding peak for Fc'(PMes$_2$)$_2$Cu$^+$ has arrived as molecular ion peak. One example is shown in the following: MS (ESI): m/z (%) 787 $[M+1]^+$. HRMS (ESI; m/z): $[M]^+$ calc for $C_{46}H_{52}CuFeP_2$, 785.21897; found 785.21842.

Fc'(PMes$_2$)$_2$.CuBr (7). Yield: 63%. ^{1}H NMR (thf-d8): δ 2.00-2.50 (brs, 36H, *o*- and *p*-C*H*$_3$ of Mes), 4.24 (brs overlapped with another brs, 8H, α- and β-H of Cp), 6.79 (brs, 8H, *m*-H of Mes). $^{13}C\{^1H\}$ NMR (thf-d8): δ 20.88 (brs, *p*-*C*H$_3$ of Mes), 73.12 (brs, α- and β-H of Cp), 78.46 (brs, ipso-C of Cp), 126.01 (s, *p*-Aryl *C* of Mes), 128.88 (s, *m*-Aryl *C* of Mes), 129.64 (s, *o*-Aryl *C* of Mes), 131.52 (brs, *ipso*-Aryl *C* of Mes). $^{31}P\{^1H\}$ NMR (thf-d8): δ -26.8. Anal. Calcd. for $C_{46}H_{52}BrCuFeP_2$: C, 63.79; H, 6.05. Found: C, 63.72; H, 5.88.

Fc'(PMes$_2$)$_2$.CuI (8). Yield: 58%. ^{1}H NMR (thf-d8): δ 2.00-2.50 (brs, 36H, *o*- and *p*-C*H*$_3$ of Mes), 4.27 (brs overlapped with another brs, 8H, α- and β-H of Cp), 6.83 (brs, 8H, *m*-H of Mes). $^{13}C\{^1H\}$ NMR (thf-d8): δ 20.87 (brs, *p*-*C*H$_3$ of Mes), 72.72 (brs, α- and β-H of Cp), 126.01 (s, *p*-Aryl *C* of Mes), 128.88 (s, *m*-Aryl *C* of Mes), 129.64 (s, *o*-Aryl *C* of Mes), 131.52 (brs, *ipso*-Aryl *C* of Mes). $^{31}P\{^1H\}$ NMR (thf-d8): δ -25.0. Anal. Calcd. for $C_{46}H_{52}CuFeIP_2$: C, 60.50; H, 5.74. Found: C, 60.72; H, 5.35.

Fc'(PMes$_2$)$_2$.Cu(BF$_4$) (9). Yield: 69%. ^{1}H NMR (CD_3CN): δ 2.00-2.50 (brs, 36H, *o*- and *p*-C*H*$_3$ of Mes), 4.24 (brs, 4H, β-H of Cp), 4.45 (brs, 4H, α -H of Cp), 6.91 (brs, 8H, *m*-H of Mes). $^{13}C\{^1H\}$ NMR (CD_3CN): δ 20.82 (s, *p*-*C*H$_3$ of Mes), 24.98 (brs, *o*-*C*H$_3$ of Mes), 73.47 (brs, α- and β-H of Cp), 78.70 (t, ipso-H of Cp, *J* = 17 Hz), 126.21 (s, *p*-Aryl *C* of Mes), 129.18 (s, *m*-Aryl *C* of Mes), 129.87 (s, *o*-Aryl *C* of Mes), 131.89 (brs, *ipso*-Aryl *C* of Mes). $^{31}P\{^1H\}$ NMR (CD_3CN): δ -27.8. $^{11}B\{^1H\}$ NMR (CD_3CN): δ -1.2. $^{19}F\{^1H\}$ NMR (CD_3CN): δ -151.9. IR (ATR) ν: 1024 (m), 1159 (m), 1444 (m), 1466 (m), 1602 (w), 2918 (w). Anal. Calcd. for $C_{46}H_{52}BCuF_4FeP_2$: C, 63.28; H, 6.00. Found: C, 63.25; H, 6.01.

Copper complexes of 3. A suspension of **3** (0.128 g, 0.20 mmol), CuX (0.2 mmol), toluene (10 mL), thf (10 mL) and CH_3CN (2 mL) was refluxed for 24 hrs. After removal of all insoluble materials by filtration, the volume of the filtrate was reduced to ca. 15 mL and analytically pure crystalline or semi-crystalline materials were obtained by slow evaporation under inert atmosphere at ambient temperature. For all the compounds, mentioned under this section, the mass spectrometric measurements gave similar data, where corresponding peak for Fc'(PMes$_2$)(PPh$_2$)Cu$^+$ has arrived as molecular ion peak. One example is shown in the following: MS (ESI): m/z (%) 701 $[M]^+$. HRMS (ESI; m/z): $[M]^+$ calc for $C_{40}H_{40}CuFeP_2$, 701.12507; found 701.12452.

Fc'(PMes$_2$)(PPh$_2$).CuBr (10). Yield: 71%. ^{1}H NMR (thf-d8): δ 2.22 (s, 6H, *p*-C*H*$_3$ of Mes), 2.32 (s, 12H, *o*-C*H*$_3$ of Mes), 4.14 (s, 2H, β-H of Cp^{PPh2}), 4.27 (pst, 2H, β-H of Cp^{PMes2}), 4.42 (s, 4H, α-H of Cp^{PPh2}), 4.49 (brs, 4H, α-H of Cp ^{PMes2}), 6.82 (brm, 4H, *m*-H of Mes), 7.38 (m, 6H, *m* and *p*-H of Ph), 7.92 (m, 4H, *o*-H of Ph). $^{13}C\{^1H\}$ NMR (thf-d8): δ 20.67 (s, *p*-*C*H$_3$ of Mes), 30.46 (s, *o*-*C*H$_3$ of Mes), 72.69 (s, β-C of Cp^{PPh2,} ^{PMes2}), 74.48 (s, α-C of Cp^{PPh2}), 77.41 (s, α-C of Cp^{PMes2}), 129.12 (d, *p*-Aryl *C* of Ph, *J* = 10 Hz), 130.67 (s, *m*-Aryl *C* of Ph), 131.63 (s, *m*-Aryl *C* of Mes), 134.95 (d, *p*-Aryl *C* of Mes, *J* = 15 Hz), 139.66 (s, *o*-Aryl *C* of Ph), 142.92 (s, *o*-Aryl *C* of Mes). $^{31}P\{^1H\}$ NMR (thf-d8): δ -31.5 (d, *P*Mes$_2$, *J* = 135 Hz), -19.3 (d, *P*Ph$_2$, *J* = 135 Hz). Anal. Calcd. for $C_{40}H_{40}BrCuFeP_2$: C, 61.44; H, 5.16. Found: C, 61.04; H, 5.15.

Fc'(PMes$_2$)(PPh$_2$).CuI (11). Yield: 74%. ^{1}H NMR (thf-d8): δ 2.22 (s, 6H, *p*-C*H*$_3$ of Mes), 2.29 (s, 12H, *o*-C*H*$_3$ of Mes), 4.12 (pst, 2H, β-H of Cp^{PPh2}), 4.26 (pst, 2H, β-H of Cp^{PMes2}), 4.42 (s, 4H, α-H of Cp^{PPh2}), 4.52 (brs, 4H, α-H of Cp ^{PMes2}), 6.82 (d, 4H, *m*-H of Mes, *J* = 3 Hz), 7.39 (m, 6H, *m* and *p*-H of Ph), 7.92 (m, 4H, *o*-H of Ph). $^{13}C\{^1H\}$ NMR (thf-d8):

δ 20.85 (s, *p*-CH_3 of Mes), 24.75 (dd, *o*-CH_3 of Mes, *J* = 9 and 1 Hz), 72.91 (m, β-C of $Cp^{PPh2, PMes2}$), 74.82 (d, α-C of Cp^{PPh2}, *J* = 10 Hz), 77.59 (m, α-C of Cp^{PMes2}), 129.28 (d, *p*-Aryl *C* of Ph, *J* = 10 Hz), 130.88 (m, *m*-Aryl *C* of Ph), 131.83 (d, *m*-Aryl *C* of Mes, *J* = 6 Hz), 135.20 (d, *p*-Aryl *C* of Mes, *J* = 15 Hz), 139.86 (s, *o*-Aryl *C* of Ph), 142.94 (d, *o*-Aryl *C* of Mes, *J* = 11 Hz). $^{31}P\{^1H\}$ NMR (thf-d8): δ -30.1 (brm, $PMes_2$), -20.2 (d, PPh_2, J = 98 Hz). Anal. Calcd. for $C_{40}H_{40}CuFeIP_2$: C, 57.95; H, 4.86. Found: C, 57.66; H, 4.90.

Fc'(PMes$_2$)(PPh$_2$).Cu(MeCN)$_2$(BF$_4$) (12). Yield: 77%. ^1H NMR (thf-d8): δ 2.08 (s, 6H, CH_3 of MeCN) 2.23 (s, 6H, *p*-CH_3 of Mes), 2.30 (s, 12H, *o*-CH_3 of Mes), 4.11 (m, 2H, β-H of Cp^{PPh2}), 4.32 (pst, 2H, β-H of Cp^{PMes2}), 4.54 (pst, 4H, α-H of Cp^{PPh2}), 4.63 (pst, 4H, α-H of Cp^{PMes2}), 6.90 (, 4H, *m*-H of Mes), 7.48 (m, 6H, *m* and *p*-H of Ph), 7.68 (m, 4H, *o*-H of Ph). $^{13}C\{^1H\}$ NMR (thf-d8): δ 1.16 (s, CH_3CN), 20.84 (s, *p*-CH_3 of Mes), 24.45 (dd, *o*-CH_3 of Mes, *J* = 11 and 1 Hz), 73.27 (d, β-C of Cp^{PPh2}, *J* = 5 Hz), 73.61 (d, β-C of Cp^{PMes2}, *J* = 6 Hz), 74.62 (d, α-C of Cp^{PPh2}, *J* = 9 Hz), 75.25 (d, ipso-C of Cp^{PPh2}, *J* = 47 Hz), 77.71 (d, α-C of Cp^{PMes2}, *J* = 14 Hz), 78.94 (d, ipso-C of Cp^{PMes2}, *J* = 39 Hz), 119.76 (s, CH_3CN), 126.06 (dd, ipso-C of Ph, *J* = 28 and 3 Hz), 130.08 (d, *p*-Aryl C of Ph, *J* = 10 Hz), 131.57 (d, *m*-Aryl C of Ph, *J* = 2 Hz), 132.02 (d, *p*-Aryl *C* of Mes, *J* = 7 Hz), 133.34 (d, ipso-C of Mes, *J* = 31 Hz), 134.70 (d, *o*-Aryl *C* of Ph, *J* = 16 Hz), 140.61 (d, *m*-Aryl *C* of Mes, *J* 2 = Hz), 142.94 (d, *o*-Aryl *C* of Mes, *J* = 11 Hz). $^{31}P\{^1H\}$ NMR (thf-d8): δ -33.5 (d, $PMes_2$, *J* = 119 Hz), -11.8 (d, PPh_2, *J* = 119 Hz). $^{11}B\{^1H\}$ NMR (thf-d8): δ -0.9. $^{19}F\{^1H\}$ NMR (thf-d8): δ -153.2. IR (ATR) ν: 1025 (s), 1034 (s), 1053 (s), 1093 (m), 1436 (m), 1600 (w), 2228 (w), 2922 (w). Anal. Calcd. for $C_{44}H_{46}BCuF_4FeN_2P_2$: C, 60.67; H, 5.32; N, 3.22. Found: C, 60.45; H, 5.34; N, 2.96.

[Fc'(PMes$_2$)$_2$.(CuBr)$_2$]$_2$ (13). A suspension of **1** (0.144 g, 0.20 mmol), CuBr (0.057 g, 0.40 mmol), toluene (10 mL), thf (15 mL) and CH_3CN (5 mL) was refluxed for 48 hrs. After removal of all insoluble materials by filtration, the volume of the filtrate was reduced to ca. 20 mL and crystalline substance along with semi-crystalline materials were obtained by slow introduction of dry pentane while kept in a double arm H-tube at ambient temperature. After several washing with a mixture of dry toluene and pentane (1:1), followed by removal of all volatiles under high vacuum (10^{-3} mbar) compound **13** was obtained in a Yield of 56%. ^1H NMR (CD_3CN): δ 2.00-2.50 (brs overlapped with another brs, 72H, *o*- and *p*-CH_3 of Mes), 4.25 (brs, 8H, α-H of Cp), 4.60 (brs, 8H, β-H of Cp), 6.88 (brs, 16H, *m*-H of Mes). $^{31}P\{^1H\}$ NMR (thf-d8): δ -26.9. $^{31}P\{^1H\}$ NMR (CD_3CN): δ -27.5. MS (MALDI): m/z (%) 850 $[M]^+$ for $[Fc'(PMes_2)_2.Cu_2]^{2+}$, 786 $[M]^+$ for $[Fc'(PMes_2)_2.Cu]^+$. Anal. Calcd. for $C_{46}H_{52}BrCuFeP_2$: C, 54.72; H, 5.19. Found: C, 54.59; H, 5.06. **Note:** Compound **13** is highly insoluble in commonly available organic solvents (including thf-d8 and CD_3CN). After a prolonged NMR experiment only ^1H (with a low S/N ratio and unresolved broad signals near to the baseline) and $^{31}P\{^1H\}$ NMR (with a satisfactory S/N ratio) could be obtained, which revealed the absence of any starting ligand (**1**) in the resulting mixture.

[Fc'(PMes$_2$)Br.CuBr]$_2$ (14). A suspension of **4** (0.107 g, 0.20 mmol), CuBr (0.029 g, 0.20 mmol), toluene (10 mL), thf (10 mL) and CH_3CN (2 mL) was refluxed for 24 hrs. After removal of all insoluble materials by filtration, the volume of the filtrate was reduced to ca. 15 mL and analytically pure crystalline materials (72%) were obtained by slow evaporation under inert atmosphere. ^1H NMR (thf-d8): δ 2.22 (brs, 12H, *p*-CH_3 of Mes), 2.29 (brs, 12H, *o*-CH_3 of Mes), 4.19 (pst, 2H, β-H of Cp^{PMes2}), 4.32 (pst, 2H, β-H of Cp^{Br}), 4.51 (s, 2H, α-H of Cp^{Br}), 4.77 (s, 2H, α -H of Cp^{PMes2}), 6.83 (d, 8H, *m*-H of Mes, *J* = 5 Hz). $^{13}C\{^1H\}$ NMR (thf-d8): 20.87(s, *p*-CH_3 of Mes), 24.77 (s, *o*-CH_3 of Mes), 70.76 (s, β-C of Cp^{Br}), 72.48 (s, α-C of Cp^{Br}), 76.10 (d, β-C of Cp^{PMes2}, *J* = 7 Hz), 77.96 (d, ipso-C of Cp^{PMes2}, *J* = 41 Hz), 78.41 (s, ipso-C of Cp^{Br}), 79.09 (brd, α-C of Cp^{PMes2}), 128.79 (d, ipso-Aryl *C* of Mes, *J* = 36 Hz), 131.74 (d, *p*-Aryl *C* of Mes, *J* = 7 Hz), 139.97 (s, *m*-Aryl *C* of Mes), 142.11 (d, *o*-Aryl *C* of Mes, *J* = 11 Hz). $^{31}P\{^1H\}$ NMR (thf-d8): δ -26.5. MS (MALDI and APCI): m/z (%) 532 (100) $[M]^+$ for starting ligand Fc'(PMes$_2$)Br and no peak for its corresponding CuBr complex **14** could be found. Anal. Calcd. for $C_{56}H_{60}Br_4Cu_2Fe_2P_2$: C, 49.70; H, 4.47. Found: C, 49.99; H, 4.43.

Catalytic reaction. A mixture of Ph–C≡C–H (0.204 g, 0.22 mL, 2 mmol, 1 equiv.), respective catalyst (mole% with respect to Cu, mentioned in Table S3, SI file), dry DMF (10 mL), and Cs_2CO_3 (0.978 g, 3 mmol, 1.5 equiv.) was degassed by three consecutive cycles of freeze (at -98 °C, MeOH and liquid N_2), pump and thaw. A balloon, filled with dry CO_2, was placed on it and the resulting reaction mixture was stirred for 36 h at rt, followed by quenching with water (20 mL). The organic layer then was separated by washing with DCM (3 × 20 mL) and the combined DCM phases were stored for further investigation. The aqueous layer was acidified with conc. HCl (up to pH 1) and extracted with EtOAc (3 × 20 mL). The resulting EtOAc phases were combined and the residual DMF was removed by washing with water (2 × 30 mL) and brine (30 mL), followed by drying upon anhydrous Na_2SO_4. Volatiles were removed under rotatory evaporator and the resulting colourless oil was subjected under controlled vacuum (5 × 10^{-2} mbar), until colourless crystals arrive (see Figure S54 in SI file). The previously collected DCM phase was then washed with water (2 × 30 mL) and brine (30 mL), dried under rotatory evaporator and finally subjected under high vacuum (10^{-3} mbar) for overnight at 40 °C. Thus-obtained yellow solids were then characterized with ^{31}P NMR, which revealed them as the remnants of catalysts.

Acknowledgement

The authors would like to thank the funding programs LOEWE and MASH for financial support. Zsolt Kelemen is grateful for the general support of Hungarian Academy of Science under the Premium Postdoctoral Research Program 2019.

Associated Content

The NMR spectra of all reported compounds, detail of the computational studies and X-ray crystallography can be found in the supporting information file, which is available free of charge on the ACS Publication website.

The CCDC deposition with number 1980151-1980158 contain the supplementary crystallographic data for compounds **3**-**6**, **10**, **12**-**14**, published in this paper, which can be obtained free of charge via emailing data_request@ccdc.cam.ac.uk, or by contacting The Cambridge Crystallographic Data Centre at 12 Union Road, Cambridge CB2 1EZ, UK; fax: +44 1223 336033.

References

1. D. E. Herbert, U. F. Mayer and I. Manners, *Angew. Chem., Int. Ed.*, 2007, **46**, 5060.
2. V. Bellas and M. Rehahn, *Angew. Chem., Int. Ed.*, 2007, **46**, 5082.
3. A. Alkan, L. Thomi, T. Gleede and F. R. Wurm, *Polym. Chem.*, 2015, **6**, 3617.
4. R. Pietschnig, *Chem. Soc. Rev.*, 2016, **45**, 5216.

5. L. Cao, I. Manners and M. A. Winnik, *Macromolecules*, 2002, **35**, 8258.
6. M. Saleem, H. Yu, L. Wang, A. Zain ul, H. Khalid, M. Akram, N. M. Abbasi and J. Huang, *Anal. Chim. Acta*, 2015, **876**, 9.
7. X. Sui, X. Feng, M. A. Hempenius and G. J. Vancso, *J. Mat. Chem. B*, 2013, **1**, 1658.
8. J. Elbert, J. Mersini, N. Vilbrandt, C. Lederle, M. Kraska, M. Gallei, B. Stühn, H. Plenio and M. Rehahn, *Macromolecules*, 2013, **46**, 4255.
9. C. Ornelas, *New J. Chem.*, 2011, **35**, 1973.
10. G. Jaouen, A. Vessieres and S. Top, *Chem. Soc. Rev.*, 2015, **44**, 8802.
11. R. L. Hailes, A. M. Oliver, J. Gwyther, G. R. Whittell and I. Manners, *Chem. Soc. Rev.*, 2016, **45**, 5358.
12. S. Takahashi and J. I. Anzai, *Materials*, 2013, **6**, 5742.
13. P. Debroy and S. Roy, *Coord. Chem. Rev.*, 2007, **251**, 203.
14. D. P. Puzzo, A. C. Arsenault, I. Manners and G. A. Ozin, *Angew. Chem., Int. Ed.*, 2009, **48**, 943.
15. A. Hor, T. S. Kim-Suan Gan, in *Ferrocenes: Homogeneous Catalysis, Organic Synthesis, Materials Science*; Ed. A. Togni, T. Hayashi, John Wiley & Sons, 2007; pp 3-104.
16. Sheau W. Chien, T. S. Andy Hor, in *Ferrocenes: Ligands, Materials and Biomolecules;* Ed. P. Štěpnička, John Wiley & Sons, 2008; pp 33-116.
17. J. J. Bishop, A. Davison, M. L. Katcher, D. W. Lichtenberg, R. E. Merrill and J. C. Smart, *J. Organomet. Chem.*, 1971, **27**, 241.
18. G. M. Whitesides, J. F. Gaasch and E. R. Stedronsky, *J. Am. Chem. Soc.*, 1972, **94**, 5258.
19. L. E. Hagopian, A. N. Campbell, J. A. Golen, A. L. Rheingold and C. Nataro, *J. Organomet. Chem.*, 2006, **691**, 4890.
20. G. Bandoli and A. Dolmella, *Coord. Chem. Rev.*, 2000, **209**, 161.
21. M. N. Birkholz, Z. Freixa and P. W. van Leeuwen, *Chem. Soc. Rev.*, 2009, **38**, 1099.
22. P. Dierkes and P. W. N. M. van Leeuwen, *J. Chem. Soc., Dalton Trans.*, 1999, 1519.
23. S. P. Thomas J. Colacot, in *Ferrocenes: Ligands, Materials and Biomolecules;* Ed. P. Štěpnička, John Wiley & Sons, 2008; pp 117-140.
24. A. Fihri, P. Meunier and J.-C. Hierso, *Coord. Chem. Rev.*, 2007, **251**, 2017.
25. P. Vosáhlo, I. Císařová and P. Štěpnička, *J. Organomet. Chem.*, 2018, **860**, 14.
26. K. Skoch, I. Cisarova, J. Schulz, U. Siemeling and P. Stepnicka, *Dalton Trans.*, 2017, **46**, 10339.
27. P. Štěpnička, in *Ferrocenes: Ligands, Materials and Biomolecules*; Ed. P. Štěpnička, John Wiley & Sons, 2008; pp 177-204.
28. W. C. Hans-Ulrich Blaser, F. Camponovo and A. Togni, in *Ferrocenes: Ligands, Materials and Biomolecules*; Ed. P. Štěpnička, John Wiley & Sons, 2008; pp 205-235.
29. P. Š. M. Lamač, in *Ferrocenes: Ligands, Materials and Biomolecules*; Ed. P. Štěpnička, John Wiley & Sons, 2008; pp 237-277.
30. U. Siemeling, in *Ferrocenes: Ligands, Materials and Biomolecules*; Ed. P. Štěpnička, John Wiley & Sons, 2008; pp 141-176.
31. A. L. Boyes, I. R. Butler and S. C. Quayle, *Tetrahedron Lett.*, 1998, **39**, 7763.
32. W. R. Cullen, T. J. Kim, F. W. B. Einstein and T. Jones, *Organometallics*, 1983, **2**, 714.
33. B. C. Hamann and J. F. Hartwig, *J. Am. Chem. Soc.*, 1998, **120**, 3694.
34. O. V. Gusev, T. y. A. Peganova, A. M. Kalsin, N. V. Vologdin, P. V. Petrovskii, K. A. Lyssenko, A. V. Tsvetkov and I. P. Beletskaya, *Organometallics*, 2006, **25**, 2750.
35. I. R. Butler, W. R. Cullen, T. J. Kim, S. J. Rettig and J. Trotter, *Organometallics*, 1985, **4**, 972.
36. T. Y. Dong and C. K. Chang, *J. Chin. Chem. Soc.*, 1998, **45**, 577.
37. A. Fihri, J. C. Hierso, A. Vion, D. H. Nguyen, M. Urrutigoïty, P. Kalck, R. Amardeil and P. Meunier, *Adv. Synth. Cat.*, 2005, **347**, 1198.
38. M. Yamashita, J. V. Cuevas Vicario and J. F. Hartwig, *J. Am. Chem. Soc.*, 2003, **125**, 16347.
39. J. C. Hierso, F. Lacassin, R. Broussier, R. Amardeil and P. Meunier, *J. Organomet. Chem.*, 2004, **689**, 766.
40. M. Laly, R. Broussier and B. Gautheron, *Tetrahedron Lett.*, 2000, **41**, 1183.
41. T. J. Colacot and H. A. Shea, *Org. Lett.*, 2004, **6**, 3731.
42. G. A. Grasa and T. J. Colacot, *Org. Lett.*, 2007, **9**, 5489.
43. T. R. Kegl, N. Palinkas, L. Kollar and T. Kegl, *Molecules*, 2018, **23**, 3176.
44. G. Cavinato and L. Toniolo, *Molecules*, 2014, **19**, 15116.
45. I. R. Butler, W. R. Cullens and T.-J. Kim, *Synth. React. Inorg. Met.-Org. Chem.*, 2006, **15**, 109.
46. L. Qin, X. Ren, Y. Lu, Y. Li and J. Zhou, *Angew. Chem., Int. Ed.*, 2012, **51**, 5915.
47. M. Ogasawara, K.-i. Takizawa and T. Hayashi, *Organometallics*, 2002, **21**, 4853.
48. L. A. Evans, N. Fey, J. N. Harvey, D. Hose, G. C. Lloyd-Jones, P. Murray, A. G. Orpen, R. Osborne, G. J. J. Owen-Smith and M. Purdie, *J. Am. Chem. Soc.*, 2008, **130**, 14471.
49. Y. Fukue, S. Oi and Y. Inoue, *J. Chem. Soc. Chem. Comm.*, 1994, 2091.
50. S. Wang, G. Du and C. Xi, *Org. Biomol. Chem.*, 2016, **14**, 3666.
51. M. Trivedi, G. Singh, A. Kumar and N. P. Rath, *Dalton Trans.*, 2015, **44**, 20874.
52. L. J. Gooßen, N. Rodríguez, F. Manjolinho and P. P. Lange, *Adv. Synth. Cat.*, 2010, **352**, 2913.
53. W. H. Wang, L. Jia, X. Feng, D. Fang, H. Guo and M. Bao, *Asian J. Org. Chem.*, 2019, **8**, 1501.
54. R. Sihler, U. Werz and H.-A. Brune, *J. Organomet. Chem.*, 1989, **368**, 213.
55. J. Roger, S. Royer, H. Cattey, A. Savateev, R. V. Smaliy, A. N. Kostyuk and J. C. Hierso, *Eur. J. Inorg. Chem.*, 2017, 330.
56. I. E. Nifant'ev, A. A. Boricenko, L. F. Manzhukova and E. E. Nifant'ev, *Phosphorus, Sulfur, and Silicon and the Relat. Elem.*, 1992, **68**, 99.
57. C. Moser, A. Orthaber, M. Nieger, F. Belaj and R. Pietschnig, *Dalton Trans.*, 2006, 3879.
58. S. Dey, J. W. Quail and J. Müller, *Organometallics*, 2015, **34**, 3039.
59. M. N. Chevykalova, *Russ. Chem. Bull., Int. Ed.* 2003, **52**, 78.
60. A. Orthaber, M. Fuchs, F. Belaj, G. N. Rechberger, C. O. Kappe and R. Pietschnig, *Eur. J. Inorg. Chem.*, 2011, 2588.
61. H. Zahra and R. Ali, *Curr. Org. Chem.*, 2018, **22**, 1589.
62. H. Schmidbaur and A. Schier, *Angew. Chem., Int. Ed.*, 2013, **52**, 176.
63. G. J. Grant, *Dalton Trans.*, 2012, **41**, 8745.
64. J. Rodrigues, M. G. Jardim, J. Figueira, M. Gouveia, H. Tomás and K. Rissanen, *New J. Chem.*, 2011, **35**, 1938.
65. R. H. Crabtree, in *Iridium Catalysis*, ed. P. G. Andersson, Springer Berlin Heidelberg, 2011, pp. 1-10.
66. Z. Qiu, S. Ren and Z. Xie, *Acc. Chem. Res.*, 2011, **44**, 299.
67. A. Sinha, T. Ghatak and J. K. Bera, *Dalton Trans.*, 2010, **39**, 11301.
68. M. Tanabe and K. Osakada, *Organometallics*, 2010, **29**, 4702.
69. E. Farnetti and S. Filipuzzi, *Inorg. Chim. Acta*, 2010, **363**, 467.
70. F. Blank and C. Janiak, *Coord. Chem. Rev.*, 2009, **253**, 827.
71. P. Mastrorilli, *Eur. J. Inorg. Chem.*, 2008, 4835.
72. G. Schmid, *Chem. Soc. Rev.*, 2008, **37**, 1909.
73. L. Pedrosa, *Synlett*, 2008, 1581.
74. G. Schmid, *Angew. Chem., Int. Ed.*, 2008, **47**, 3496.
75. A. B. Chaplin, *CHIMIA Int. J. Chem.*, 2008, **62**, 217.
76. C. Lau, S. Ng, G. Jia and Z. Lin, *Coord. Chem. Rev.*, 2007, **251**, 2223.
77. S. Krompiec, N. Kuźnik, M. Krompiec, R. Penczek, J. Mrzigod and A. Tórz, *J. Mol. Catal. A: Chem.*, 2006, **253**, 132.
78. D. W. Allen and B. F. Taylor, *J. Chem. Soc., Dalton Trans.*, 1982, 51.
79. P. Arsenyan, A. Petrenko, K. Oberte and S. Belyakov, *Chem. Heterocycl. Compd.*, 2012, **48**, 1263.
80. F. N. Blanco, L. E. Hagopian, W. R. McNamara, J. A. Golen, A. L. Rheingold and C. Nataro, *Organometallics*, 2006, **25**, 4292.
81. M. Necas, M. Beran, J. Derek Woollins and J. Novosad, *Polyhedron*, 2001, **20**, 741.
82. K. D. Reichl, C. L. Mandell, O. D. Henn, W. G. Dougherty, W. Scott Kassel and C. Nataro, *J. Organomet. Chem.*, 2011, **696**, 3882.

View Article Online
DOI: 10.1039/D0DT00941E

View Article Online
DOI: 10.1039/D0DT00941E

83. S. Isenberg, S. Weller, D. Kargin, S. Valic, B. Schwederski, Z. Kelemen, C. Bruhn, K. Krekic, M. Maurer, C. M. Feil, M. Nieger, D. Gudat, L. Nyulaszi and R. Pietschnig, *Chem. Open*, 2019, **8**, 1235.
84. A. Lik, D. Kargin, S. Isenberg, Z. Kelemen, R. Pietschnig and H. Helten, *Chem. Comm.*, 2018, **54**, 2471.
85. A. Jakob, P. Ecorchard, M. Linseis, R. F. Winter and H. Lang, *J. Organomet. Chem.*, 2009, **694**, 655.
86. F. Barrière, R. U. Kirss and W. E. Geiger, *Organometallics*, 2005, **24**, 48.
87. P. Zanello, G. Opromolla, G. Giorgi, G. Sasso and A. Togni, *J. Organomet. Chem.*, 1996, **506**, 61.
88. C. L. Mandell, S. S. Kleinbach, W. G. Dougherty, W. S. Kassel and C. Nataro, *Inorg. Chem.*, 2010, **49**, 9718.
89. A. Orthaber, R. H. Herber and R. Pietschnig, *J. Organomet. Chem.*, 2012, **719**, 36.
90. M. Trivedi, S. K. Ujjain, G. Singh, A. Kumar, S. K. Dubey and N. P. Rath, *J. Organomet. Chem.*, 2014, **772-773**, 202-209.
91. D. Li, Y.-F. Luo, T. Wu and S. W. Ng, *Acta Cryst. E*, 2004, **60**, m927.
92. M. Trivedi, R. Nagarajan, A. Kumar, N. P. Rath and P. Valerga, *Inorg. Chim. Acta*, 2011, **376**, 549.
93. S. P. Neo, Z.-Y. Zhou, T. C. W. Mak and T. S. A. Hor, *J. Chem. Soc., Dalton Trans.*, 1994, 3451.
94. P. Pinto, M. J. Calhorda, V. Félix, T. Avilés and M. G. B. Drew, *Monatsh. Chem.*, 2000, **131**, 1253.
95. C. Di Nicola, Effendy, C. Pettinari, B. W. Skelton, N. Somers and A. H. White, *Inorg. Chim. Acta*, 2005, **358**, 695.
96. J. Díez, M. P. Gamasa, J. Gimeno, M. Lanfranchi and A. Tiripicchio, *J. Organomet. Chem.*, 2001, **637-639**, 677.
97. M. Trivedi, G. Singh, A. Kumar and N. P. Rath, *Dalton Trans.*, 2014, **43**, 13620.
98. P. Sameer Prasad, M. K. Pandey and M. S. Balakrishna, *Polyhedron*, 2019, **158**, 173.
99. S. K. Gibbons, R. P. Hughes, D. S. Glueck, A. T. Royappa, A. L. Rheingold, R. B. Arthur, A. D. Nicholas and H. H. Patterson, *Inorg. Chem.*, 2017, **56**, 12809.
100. K. M. Gramigna, J. V. Oria, C. L. Mandell, M. A. Tiedemann, W. G. Dougherty, N. A. Piro, W. S. Kassel, B. C. Chan, P. L. Diaconescu and C. Nataro, *Organometallics*, 2013, **32**, 5966.
101. H. Tran-Vu and O. Daugulis, *ACS Catal.*, 2013, **3**, 2417.
102. L. Dang, Z. Lin and T. B. Marder, *Organometallics*, 2010, **29**, 917.
103. S. S. Zigler, L. M. Johnson and R. West, *J. Organomet. Chem.*, 1988, **341**, 187.
104. X. Wu, W. Zhang, X. Zhang, N. Ding and T. S. A. Hor, *Eur. J. Inorg. Chem.*, 2015, **2015**, 876.
105. J. Campos, M. F. Espada, J. Lopez-Serrano and E. Carmona, *Inorg. Chem.*, 2013, **52**, 6694.
106. G. R. Fulmer, A. J. M. Miller, N. H. Sherden, H. E. Gottlieb, A. Nudelman, B. M. Stoltz, J. E. Bercaw and K. I. Goldberg, *Organometallics*, 2010, **29**, 2176.
107. G. M. Sheldrick, *Acta Cryst. A*, 2008, **64**, 112.
108. C. F. Macrae, P. R. Edgington, P. McCabe, E. Pidcock, G. P. Shields, R. Taylor, M. Towler and J. van de Streek, *J. Appl. Cryst.*, 2006, **39**, 453.
109. A. L. Spek, *Acta Cryst. C*, 2015, **71**, 9.
110. C. F. Macrae, I. J. Bruno, J. A. Chisholm, P. R. Edgington, P. McCabe, E. Pidcock, L. Rodriguez-Monge, R. Taylor, J. van de Streek and P. A. Wood, *J. Appl. Cryst.*, 2008, **41**, 466.
111. I. Noviandri, K. N. Brown, D. S. Fleming, P. T. Gulyas, P. A. Lay, A. F. Masters and L. Phillips, *J. Phys. Chem. B*, 1999, **103**, 6713.

View Article Online
DOI: 10.1039/D0DT00941E

Table of contents entry

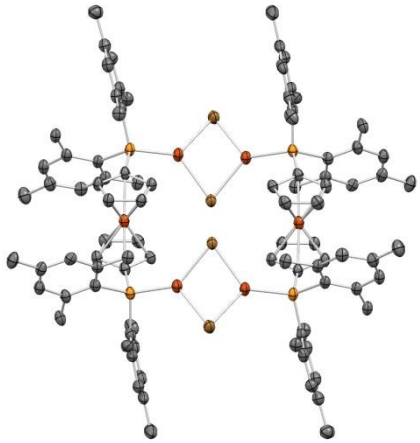

Bulky dppf analogs are reported for which the donor properties and coordination behavior has been explored and tested in a catalytic model reaction.